# Exploring the perspectives of superconducting materials in SRF for quantum sensing


*Enrico Silva*

**INFN/University Roma Tre**

enrico.silva@uniroma3.it

*A. Alimenti, G. Mota, A. Magalotti, N. Pompeo, K. Torokhtii, P. Vidal Garcìa*

*M. Bertucci, E. Chyhyrynets, D. Di Gioacchino, C. Gatti, G. Ghigo, D. Torsello, C. Pira (P.I.)*

*G. Celentano, A. Mancini, A. Masi, A. Vannozzi*

*S. Posen*

*V. Braccini, E. Bellingeri, A. Leveratto, F. Loria*

*M. Putti*


SAMARA

Superconducting Alternative Materials for Accelerating cavities and haloscope Resonators for Axions

PRIN IRONMOON

PRIN HIBiSCUS

ADDENDUM
FCC-GOV-CC-0218
(KE5084/ATS)

# Outline

- Motivation: Search for axions → Haloscopes
- Cavity haloscopes → surface impedance in dc magnetic fields → the problem(s)
- Surface impedance in superconductors in dc fields: vortex motion, geometric effect, nontrivial role of λ (and deconstruction of "well known" rules of thumb)
- Experimental technique: two-tone dielectric loaded resonator
- Results: NbTi, a case study. Fe(Se,Te). YBCO. ($Nb_3Sn$)
- Perspective superconductors for Haloscopes
- Summary

# Search for axions: microwave Haloscopes (High-Q cavities)

**Inverse Primakov effect** $\mathcal{L}_{a\gamma\gamma} = -g_{a\gamma\gamma} a \vec{E}_{rf} \cdot \vec{B}$

Peccei, Quinn
PRL 38 1440 (1977),
PRD 16 1791 (1977)

P. Sikivie
PRD 32 2988 (1985)

D. Kim et al,
J. Cosmol.
Astropart. Phys.
2020 66 (2020)

Semertzidis, Youn
Sci. Adv. 8
eabm9928 (2022)

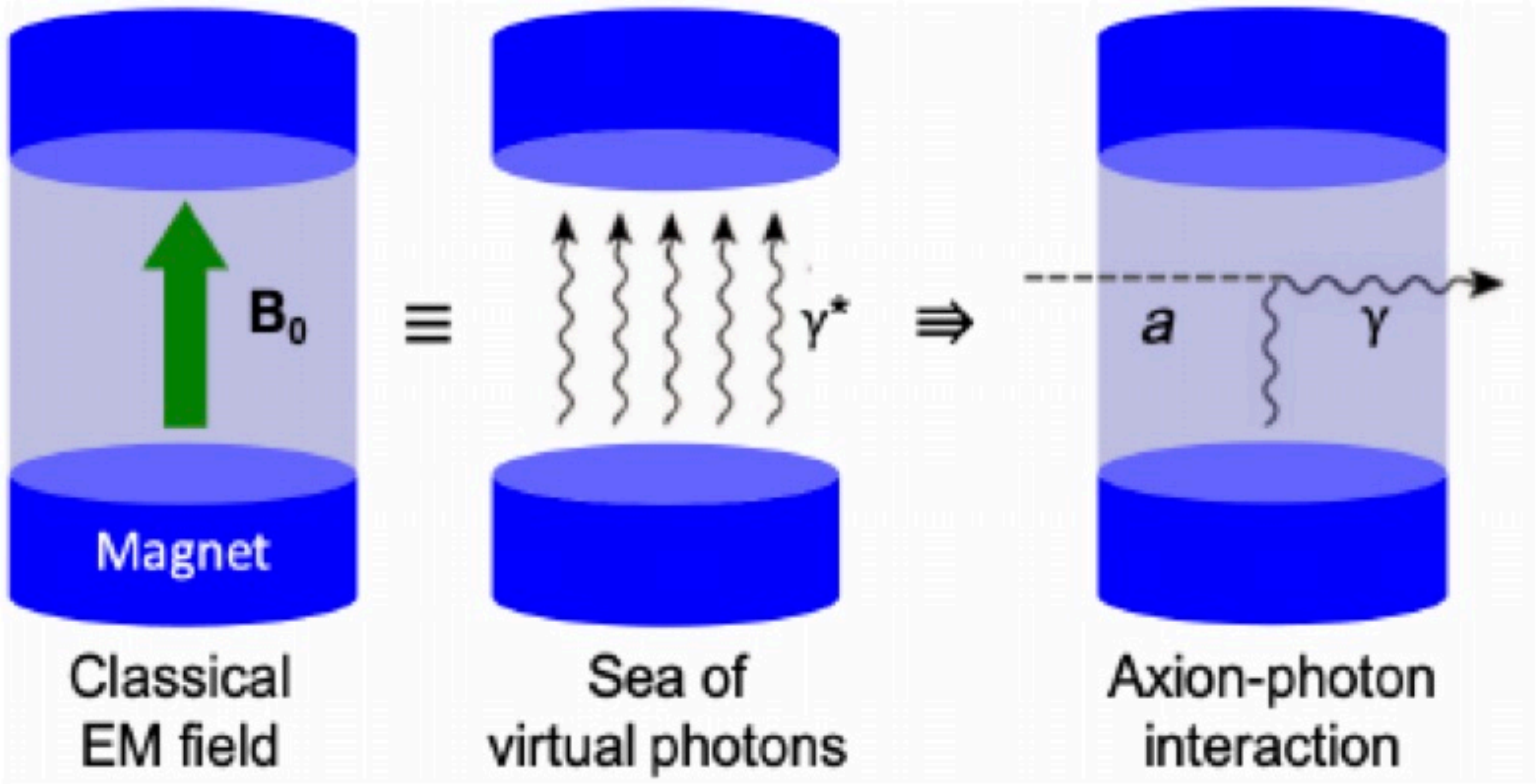


$$P_{a\to\gamma\gamma} \propto \left( B^2 c_{nl} V \frac{Q_{nm} Q_a}{Q_{nm} + Q_a} \right) (g_{a\gamma\gamma}^2)$$

Figure of merit:
***Q·B²***

- High Q resonant cavities → **Superconductor**
- Axion mass → **microwaves**
- <u>in high magnetic fields *B*</u> → <u>**vortex motion!**</u>
- low *T* (~ 0.1÷1 K) → **any superconductor**
- large, curved surfaces → **deposition issues**

beware!

# High-Q cavities: low surface resistance

**Figure of merit:**
***Q·B²***

$$Q \propto \frac{1}{R_s}$$

Surface resistance

- High Q resonant cavities → **Superconductor**
- Axion mass → **microwaves**
- <u>in high magnetic fields *B*</u> → <u>**vortex motion!**</u>
- low *T* (~ 0.1÷1 K) → **any superconductor**
- large, curved surfaces → **deposition issues**

**beware!**

# High-Q cavities: low surface resistance

**Figure of merit:**
**$Q \cdot B^2$**

$$Q \propto \frac{1}{R_s}$$

Surface resistance

$R_s$:
- geometry $B$ - $J_{mw}$
- quasiparticle conductivity
- impurities
- vortex motion
- London penetration depth

- High Q resonant cavities → **Superconductor**
- Axion mass → **microwaves**
- in high magnetic fields $B$ → **vortex motion!**
- low $T$ (~ 0.1÷1 K) → **any superconductor**
- large, curved surfaces → **deposition issues**

beware!

# Surface impedance in a dc magnetic field

$$Z_s = \frac{E_{//}}{H_{//}} = R_s + iX_s \; = \; Z_s(\sigma_{2fl}, \rho_v, R_{res})$$

$\omega = 2\pi\nu$

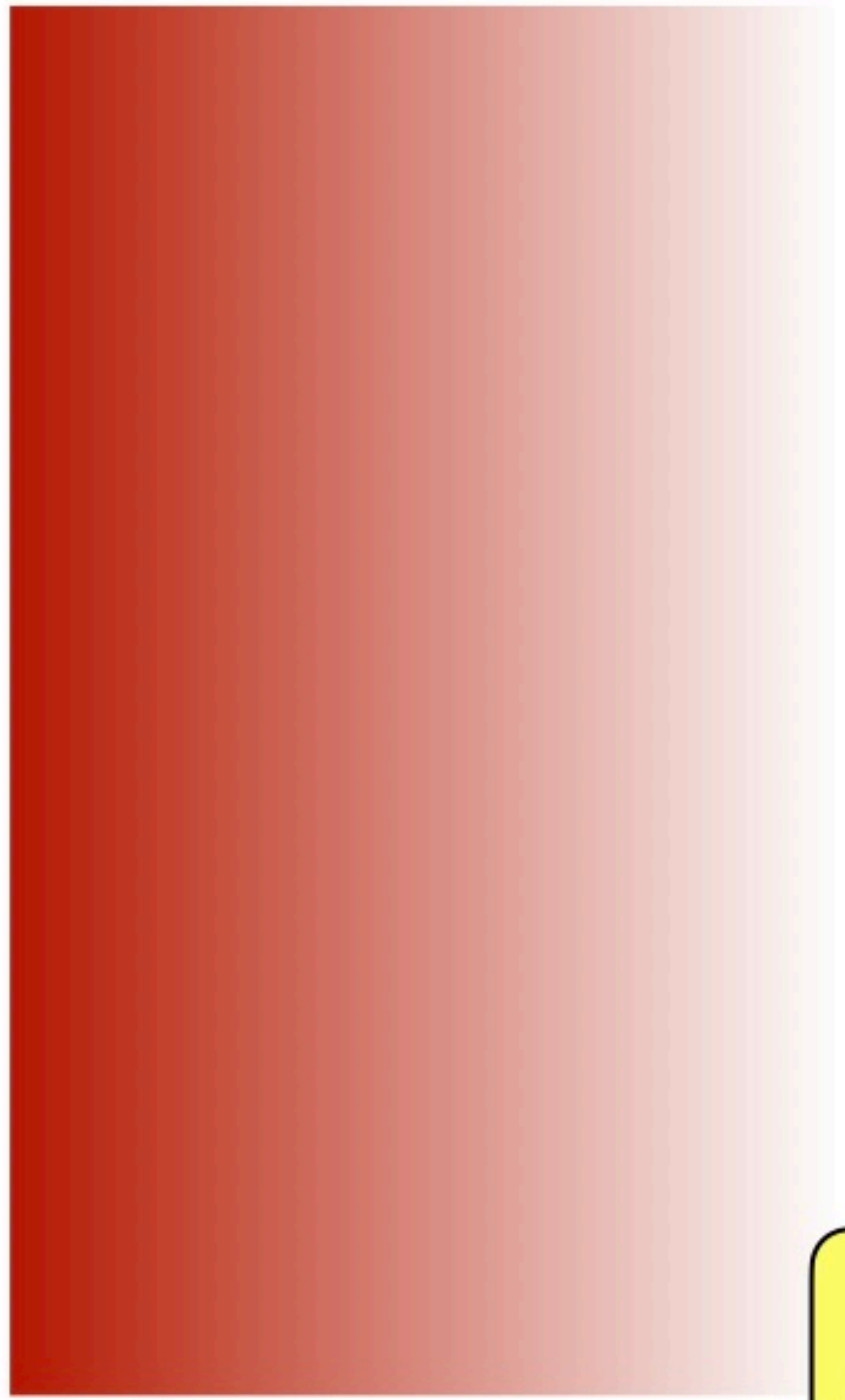

**Two fluid conductivity**

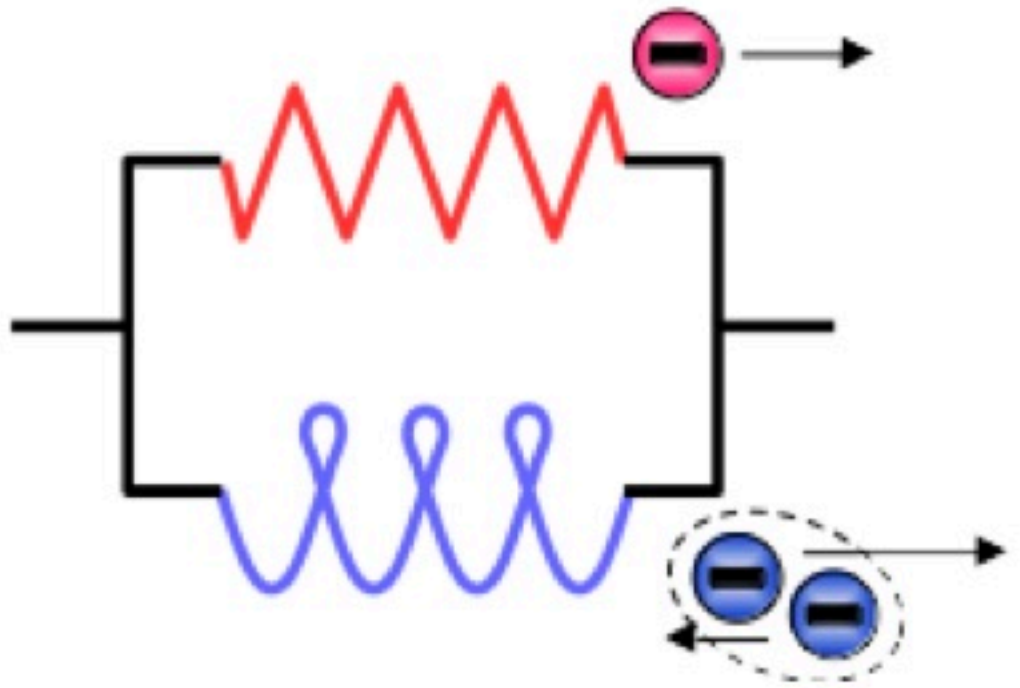

$$\sigma_1 - \mathrm{i}\sigma_2 = \frac{n_n e^2 \tau}{m} - \mathrm{i}\frac{1}{\omega\mu_0\lambda^2}$$

**All quantities depend on *B***

**vortex motion resistivity**

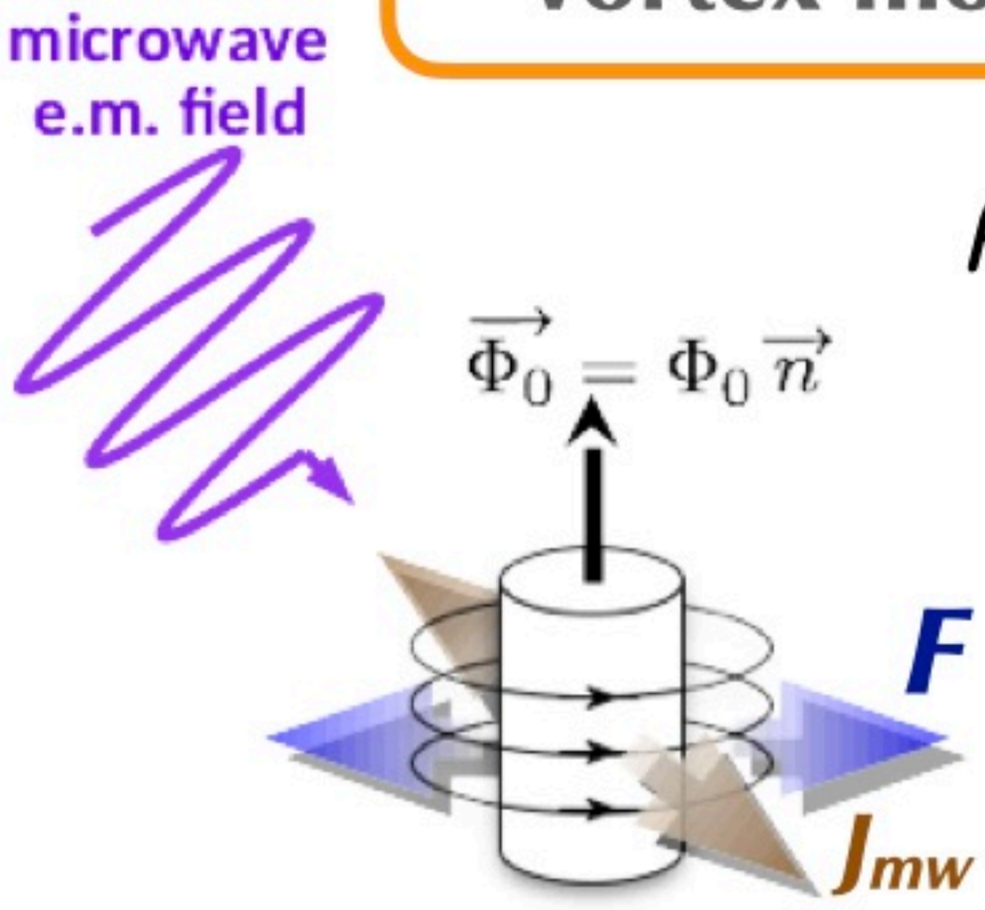


$$\rho_v = \rho_{v1} + \mathrm{i}\rho_{v2}$$

$$\boldsymbol{F} \propto J_{mw} \times \widehat{\Phi}_0$$

$$\tilde{\rho} = \frac{\rho_v + \mathrm{i}\frac{1}{\sigma_2}}{1 + \mathrm{i}\frac{\sigma_1}{\sigma_2}}$$

Coffey, Clem *PRL* **67** (1991)

# Surface impedance in a dc magnetic field

$$Z_s = \sqrt{\mathrm{i}\frac{\omega\mu_0}{\sigma}} = \sqrt{\mathrm{i}\omega\mu_0\tilde{\rho}}$$

$$\tilde{\rho} = \frac{\rho_v + \mathrm{i}\frac{1}{\sigma_2}}{1 + \mathrm{i}\frac{\sigma_1}{\sigma_2}}$$

$$\sigma_1 - \mathrm{i}\sigma_2 = \frac{n_n e^2 \tau}{m} - \mathrm{i}\frac{1}{\omega\mu_0\lambda^2}$$

$$\rho_v = \rho_{v1} + \mathrm{i}\rho_{v2}$$

**vortex motion resistivity, "the new actor in town"**

# Surface impedance in a dc magnetic field

$$Z_s = \sqrt{\mathrm{i}\frac{\omega\mu_0}{\sigma}} = \sqrt{\mathrm{i}\omega\mu_0\tilde{\rho}}$$

$$\tilde{\rho} = \frac{\rho_v + \mathrm{i}\frac{1}{\sigma_2}}{1 + \mathrm{i}\frac{\sigma_1}{\sigma_2}}$$

$$\sigma_1 - \mathrm{i}\sigma_2 = \frac{n_n e^2 \tau}{m} - \mathrm{i}\frac{1}{\omega\mu_0\lambda^2}$$

$$\rho_v = \rho_{v1} + \mathrm{i}\rho_{v2}$$

**vortex motion resistivity, “the new actor in town”**

**Deconstruction of “well known” rules of thumb**

Assume to be far from the transition line: $T \ll T_c$ → $R_s \simeq \frac{\Re[\tilde{\rho}]}{2\lambda}$

**Zero field, B=0**

$$Z_s \simeq \frac{1}{2}\sigma_1\omega^2\mu_0^2\lambda^3 + \mathrm{i}\omega\mu_0\lambda$$

$$R_s \simeq \frac{1}{2}\sigma_1\omega^2\mu_0^2\lambda^3 \ (+R_{res})$$

# Surface impedance in a dc magnetic field

$$Z_s = \sqrt{\mathrm{i}\frac{\omega\mu_0}{\sigma}} = \sqrt{\mathrm{i}\omega\mu_0\tilde{\rho}}$$

$$\tilde{\rho} = \frac{\rho_v + \mathrm{i}\frac{1}{\sigma_2}}{1 + \mathrm{i}\frac{\sigma_1}{\sigma_2}}$$

$$\sigma_1 - \mathrm{i}\sigma_2 = \frac{n_n e^2 \tau}{m} - \mathrm{i}\frac{1}{\omega\mu_0\lambda^2}$$

$$\rho_v = \rho_{v1} + \mathrm{i}\rho_{v2}$$

**vortex motion resistivity, "the new actor in town"**

$\rho_{v_1}$ dominant at even few mT

## Deconstruction of "well known" rules of thumb

Assume to be far from the transition line: $T \ll T_c$, $B \ll B_{c2}$ → $R_s \simeq \frac{\Re[\tilde{\rho}]}{2\lambda}$

**Zero field, B=0**

$$Z_s \simeq \frac{1}{2}\sigma_1\omega^2\mu_0^2\lambda^3 + \mathrm{i}\omega\mu_0\lambda$$

$$R_s \simeq \frac{1}{2}\sigma_1\omega^2\mu_0^2\lambda^3 \ (+R_{res})$$

**Mixed state, B≠0**

$$Z_s \simeq \frac{1}{2\lambda}\rho_v(\omega, B, T) + \mathrm{i}\omega\mu_0\lambda$$

$$R_s \simeq \frac{1}{2\lambda}\rho_{v1}(\omega, B, T)$$

- No $R_s \propto \omega^2$ dependence
- $\lambda$ large → *decreases* $R_s$
- $R_{res}$ irrelevant

physics of vortex motion resistivity required

# Microwave vortex complex resistivity

- **vortex ↔ particle in a pinning potential landscape subjected to the Lorentz force**

- **Tiny vortex oscillations (< 1nm)**
- **Local pinning potential**
- **Quasi-equilibrium vortex matter**

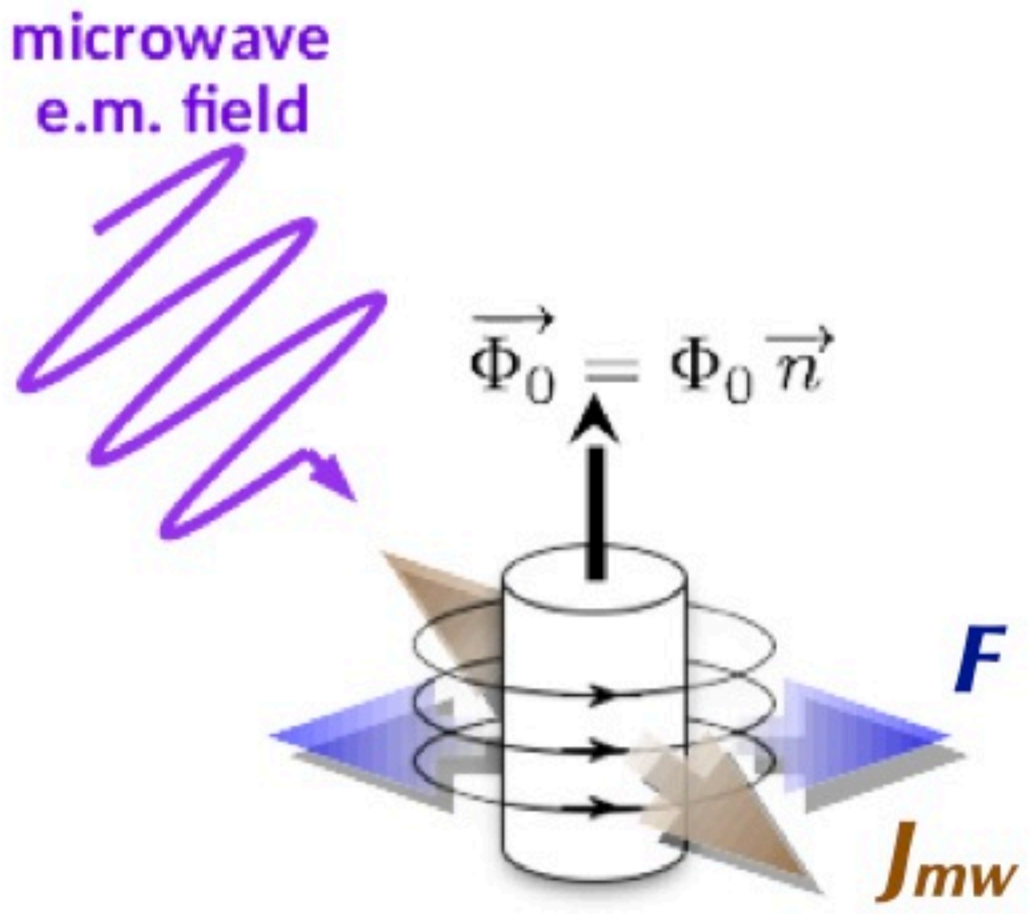


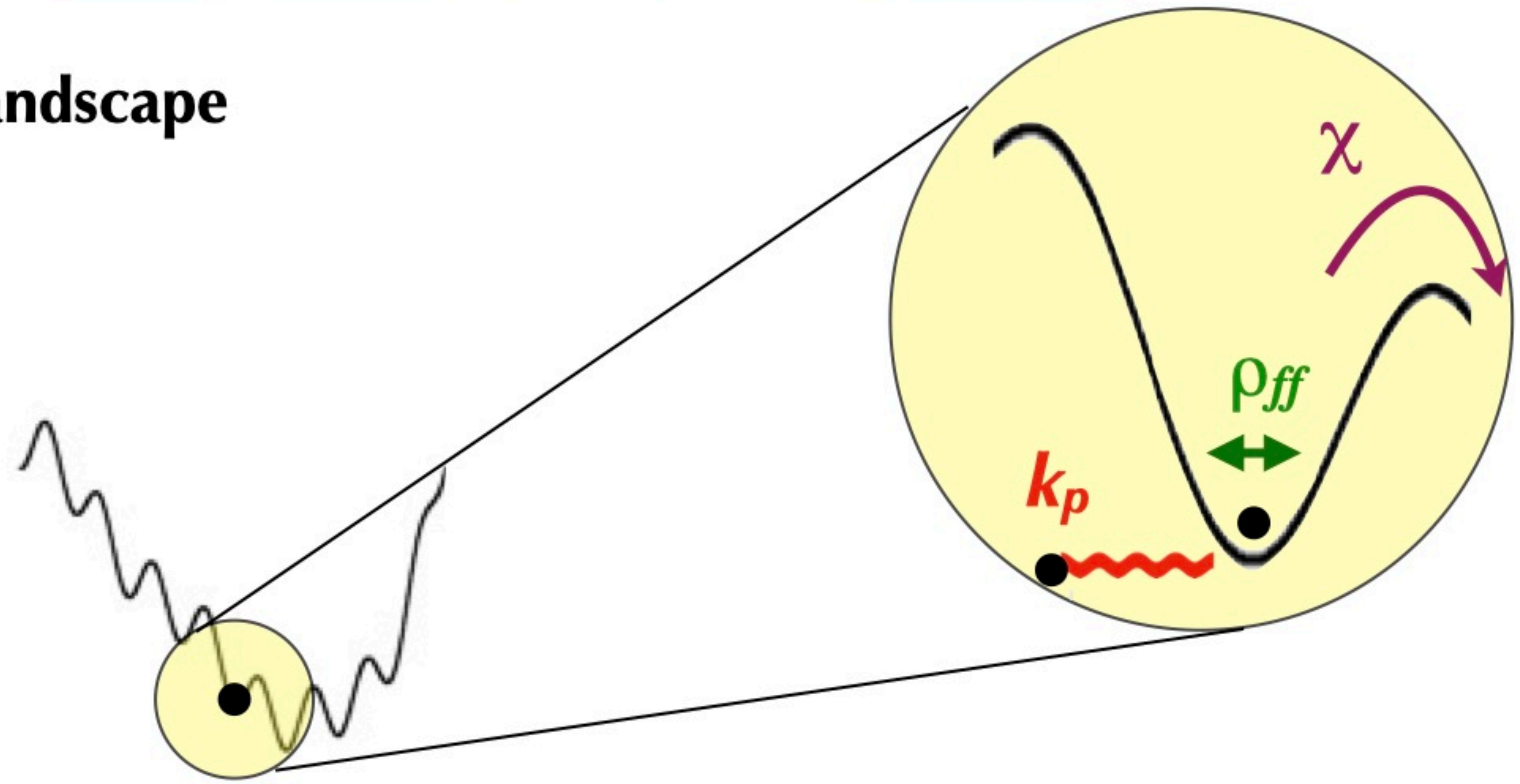


$$\rho_{v1}(H) + \mathrm{i}\rho_{v2}(H) = \rho_{ff} \frac{\chi + \mathrm{i}\frac{\nu}{\nu_0}}{1 + \mathrm{i}\frac{\nu}{\nu_0}}$$

Gittleman, Rosenblum *PRL* **16** (1966); Coffey, Clem *PRL* **67** (1991); Brandt *PRL* **67** (1991); Placais et al, *PRB* **54** (1996); N. Pompeo, E.Silva *PRB* **78** 094503 (2008); E.Silva, N. Pompeo, O. Dobrovolskiy, *Phys. Sci. Rev.* **2** 20178004 (2017) - overview

# Microwave vortex complex resistivity

- **vortex ↔ particle in a pinning potential landscape subjected to the Lorentz force**

- **Tiny vortex oscillations (< 1nm)**
- **Local pinning potential**
- **Quasi-equilibrium vortex matter**

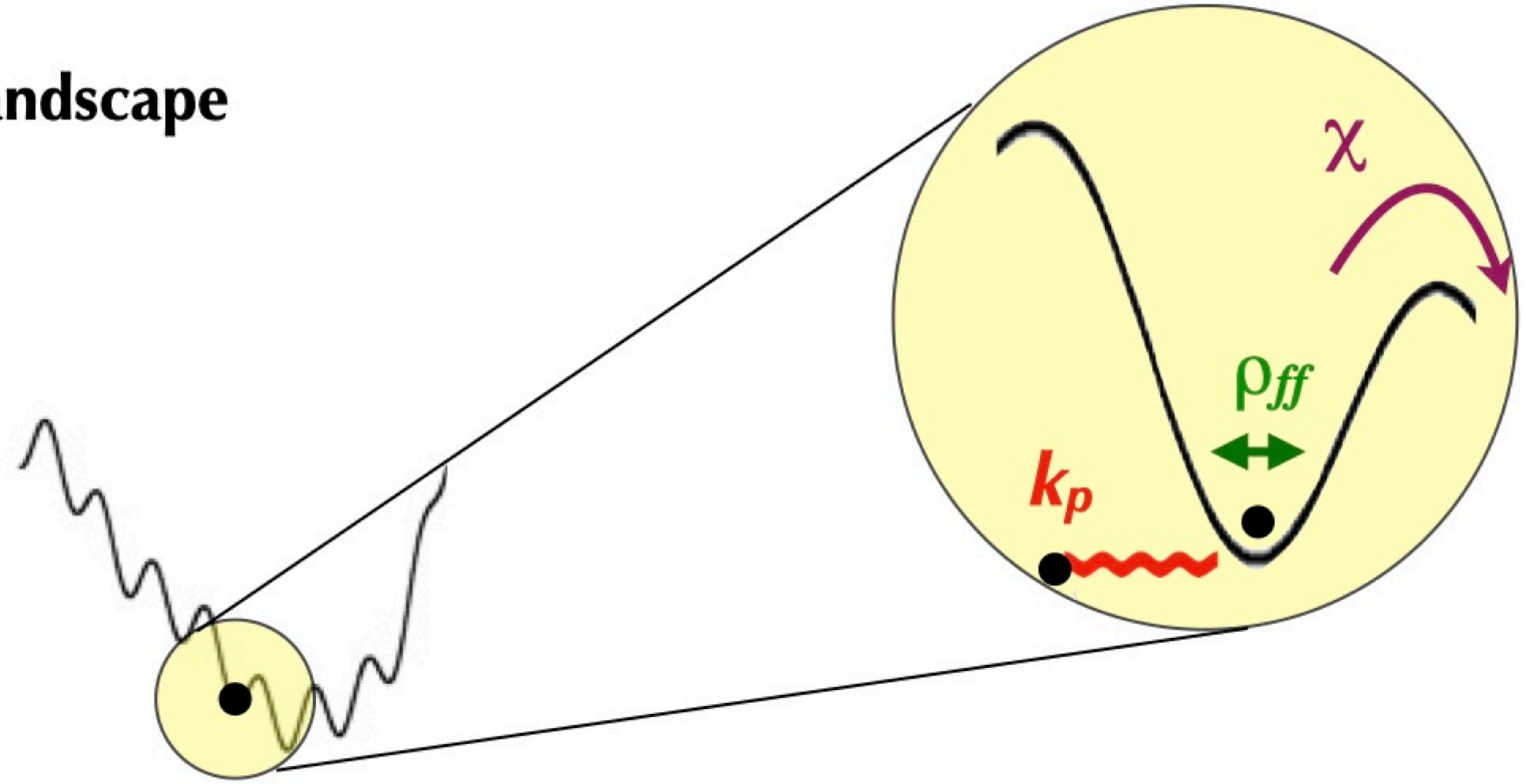


**flux-flow resistivity** $\rho_{ff}$,
**pinning constant** $k_p$,
**crossover frequency** $\nu_0$
**creep factor** $\chi$.
(low $T$: $\chi = 0$)

$$\rho_{v1}(H) + \mathrm{i}\rho_{v2}(H) = \rho_{ff}\frac{\chi + \mathrm{i}\frac{\nu}{\nu_0}}{1 + \mathrm{i}\frac{\nu}{\nu_0}}$$

$k_p \oplus \rho_{ff} \oplus \chi$ → $\nu_0$

Gittleman, Rosenblum *PRL* **16** (1966); Coffey, Clem *PRL* **67** (1991); Brandt *PRL* **67** (1991); Placais et al, *PRB* **54** (1996); N. Pompeo, E.Silva *PRB* **78** 094503 (2008); E.Silva, N. Pompeo, O. Dobrovolskiy, *Phys. Sci. Rev.* **2** 20178004 (2017) - overview

# Microwave vortex complex resistivity

$\nu_0 \approx \nu_p$, Depinning frequency.
Figure of merit for applications

$$\rho_{v1}(H) + \mathrm{i}\rho_{v2}(H) = \rho_{ff} \frac{\chi + \mathrm{i}\frac{\nu}{\nu_0}}{1 + \mathrm{i}\frac{\nu}{\nu_0}}$$

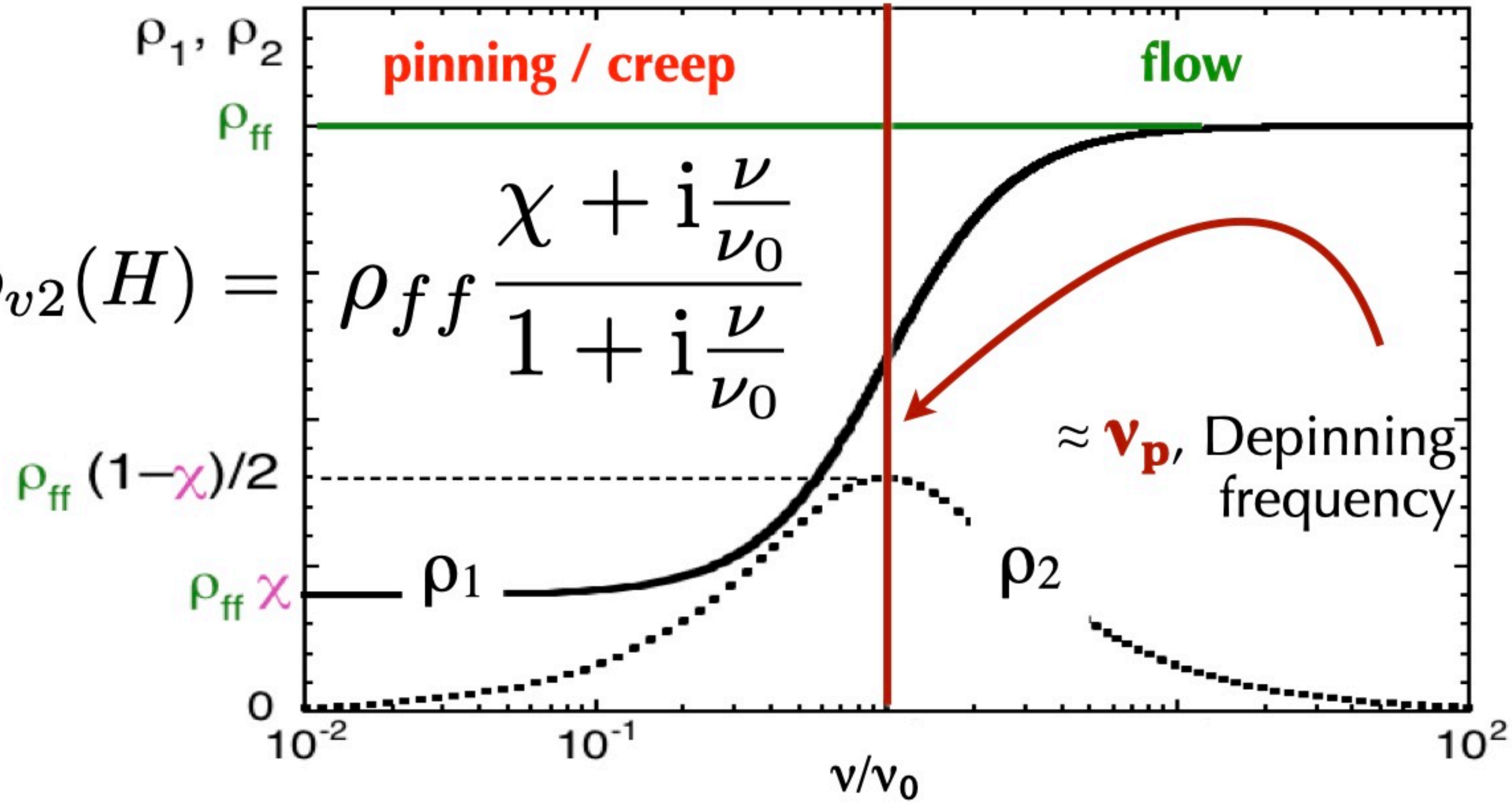


**flux-flow resistivity** $\rho_{ff}$,
**pinning constant** $k_p$,
**crossover frequency** $\nu_0$
**creep factor** $\chi$.
(low $T$: $\chi = 0$)

Gittleman, Rosenblum *PRL* **16** (1966); Coffey, Clem *PRL* **67** (1991); Brandt *PRL* **67** (1991); Placais et al, *PRB* **54** (1996);
N. Pompeo, E.Silva *PRB* **78** 094503 (2008); E.Silva, N. Pompeo, O. Dobrovolskiy, *Phys. Sci. Rev.* **2** 20178004 (2017) - overview

# Geometry: fluxons are flexible!

Force on fluxons: $F \propto J_{mw} \times \widehat{\Phi}_0$

Ideal haloscope configuration: $J_{mw} // \widehat{\Phi}_0 \Rightarrow \rho_v = 0$

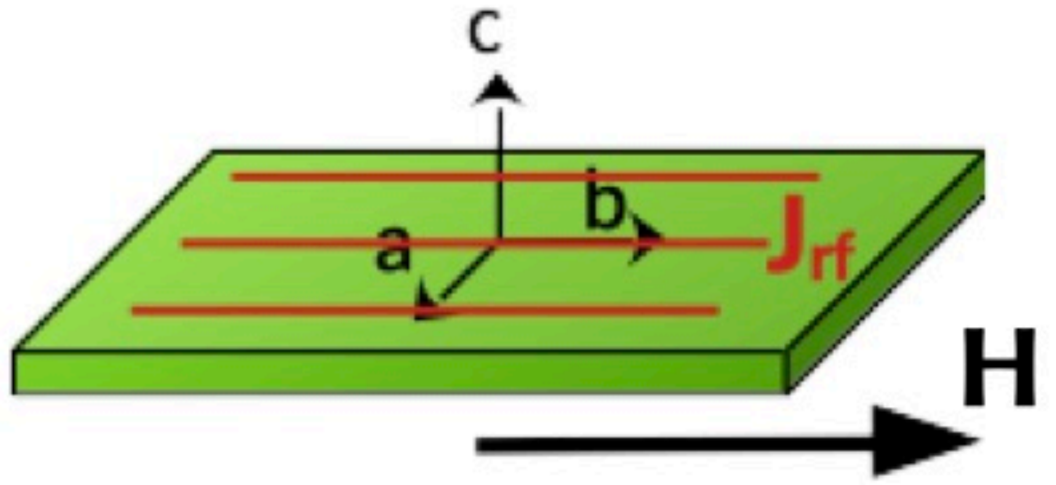


Flexible fluxons:

a contribution always exists, and depends on:

- kind of pinning (point, linear…)
- temperature
- material anisotropy (anisotropic materials → more flexible fluxons)
- fluxon stiffness (coherence length, penetration depth)

$$\rho_v = c_{ff}\ \rho_{ff} \frac{\chi + \mathrm{i}\frac{\nu}{\nu_0}}{1 + \mathrm{i}\frac{\nu}{\nu_0}}$$

$c_{ff}$: alignment factor

$c_{ff} = 0$: ideal force-free configuration

$c_{ff} = 1$: $J_{mw} \perp H$

# To predict the performances of a superconductor…

$T \ll T_c$
$B \ll B_{c2}$

$$R_s \simeq \frac{1}{2}\, c_{ff}\, \rho_{ff}\, \frac{1}{1+(\nu_0/\nu)^2}\, \frac{1}{\lambda}$$

$c_{ff}$: theoretical evaluations: only oversimplified models, many material parameters. Measure?

$\rho_{ff}$, $\nu_0$: can be measured with $H \perp J_{mw}$

$\lambda$: can be measured/ taken from literature

Note: formula is a limiting expression. Calculations were made with the full expressions

# Technique: measuring the surface impedance whence the vortex motion parameters

# Microwave technique: dielectric loaded resonator

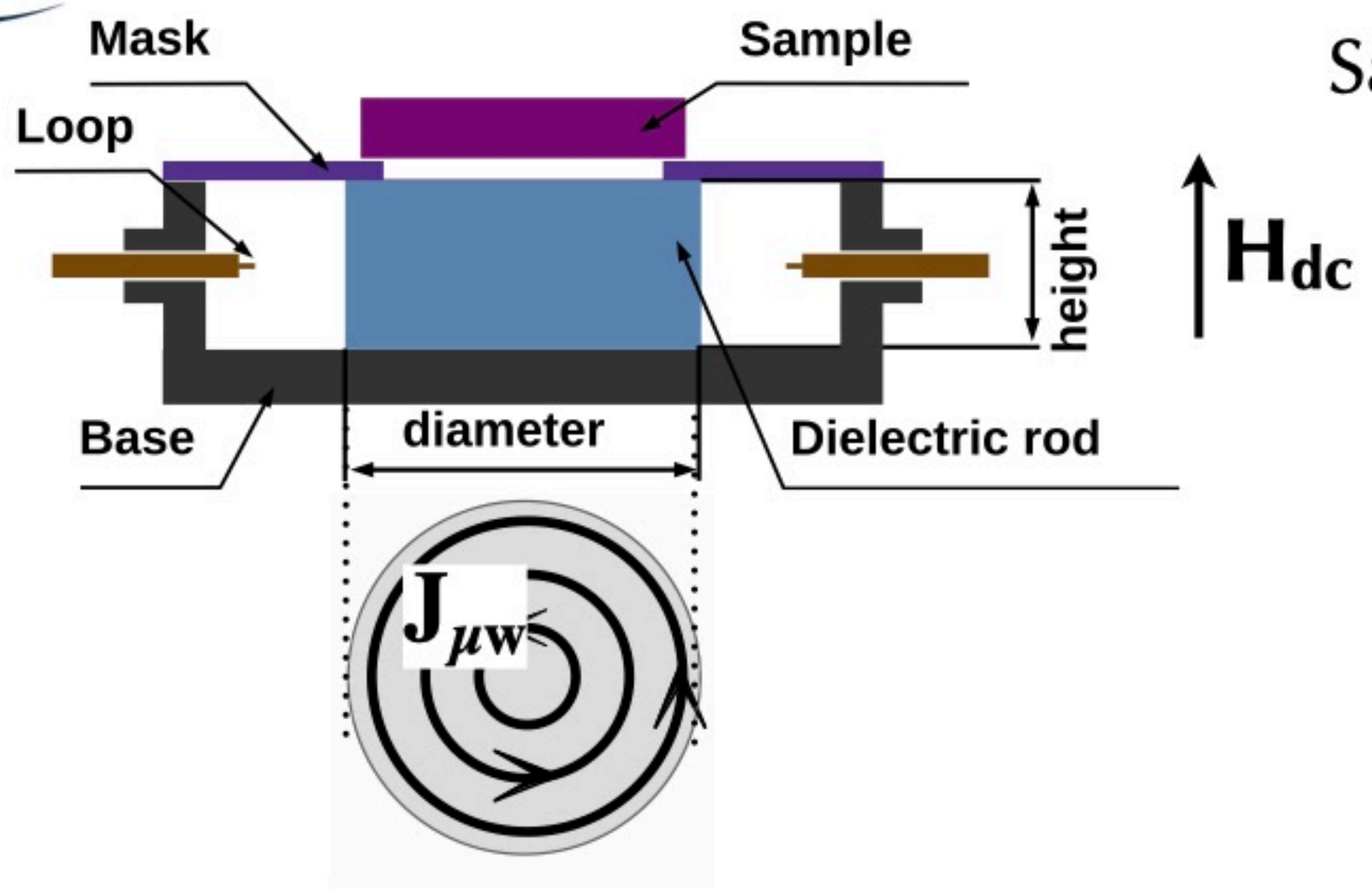


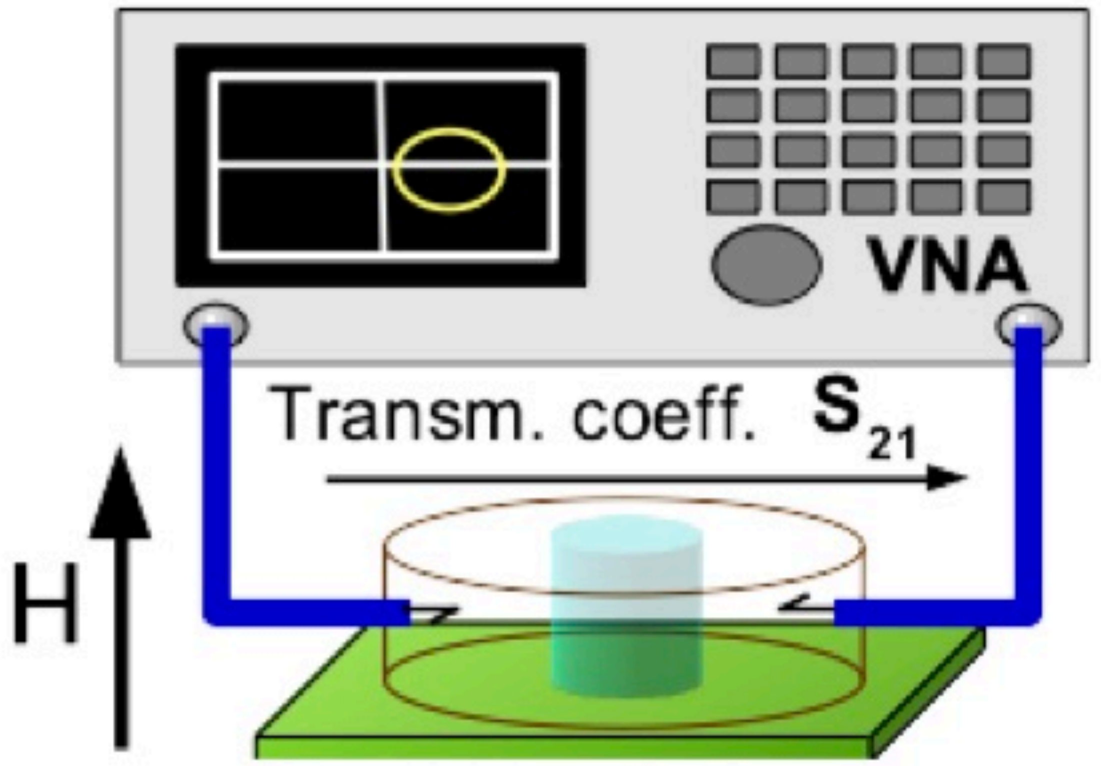


Sapphire loaded resonator

Probing area
Ø ≤ 20 mm

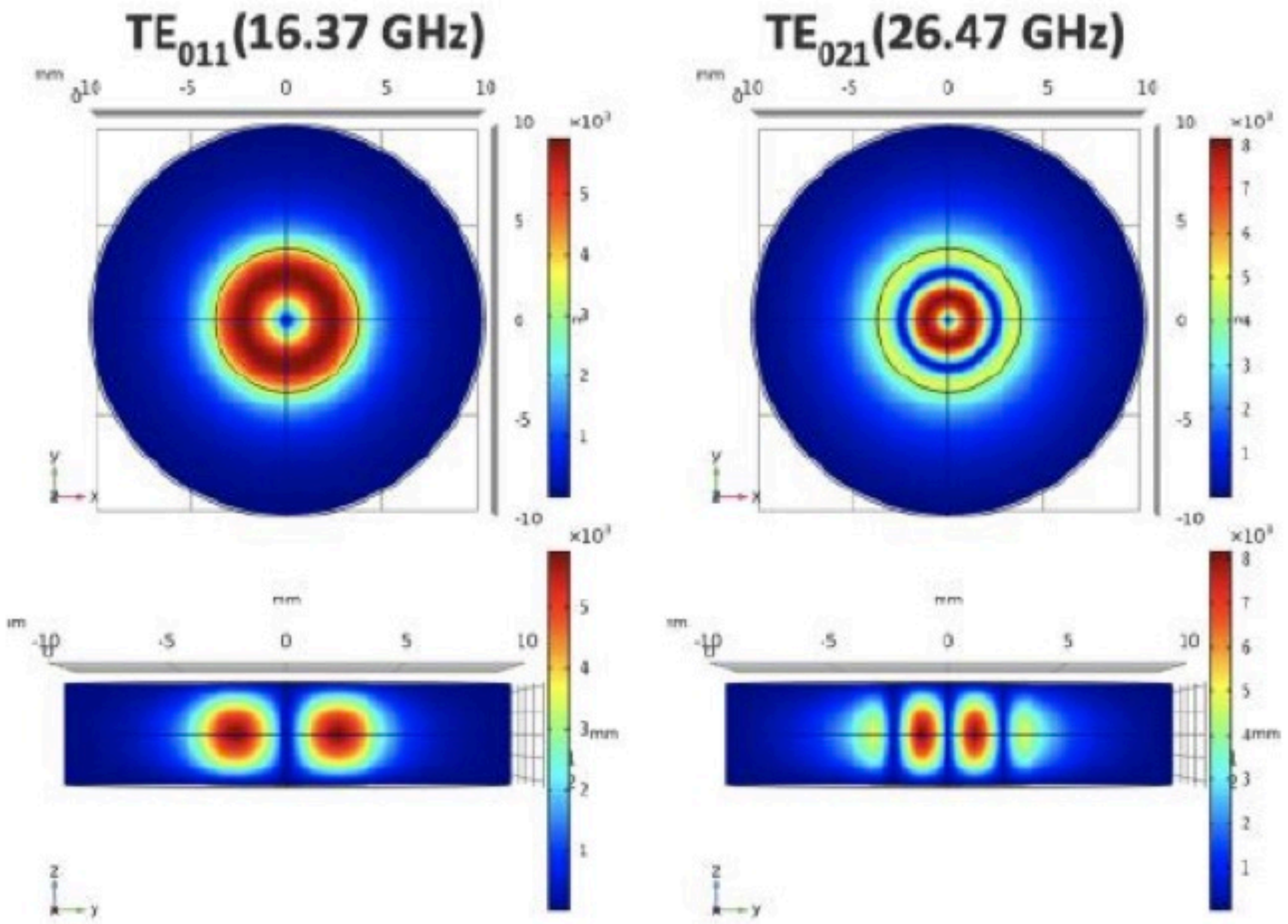


K. Torokhtii et al J. Phys.: Conf. Ser. 1065 052027 2018
A. Alimenti et al., Meas. Sci. Technol., 30 065601 2019

N. Pompeo et al., Measurement 184 109937 2021
A. Alimenti et al., IEEE Instrum. Meas. Magazine 24 12 2021

# Microwave technique: dielectric loaded resonator

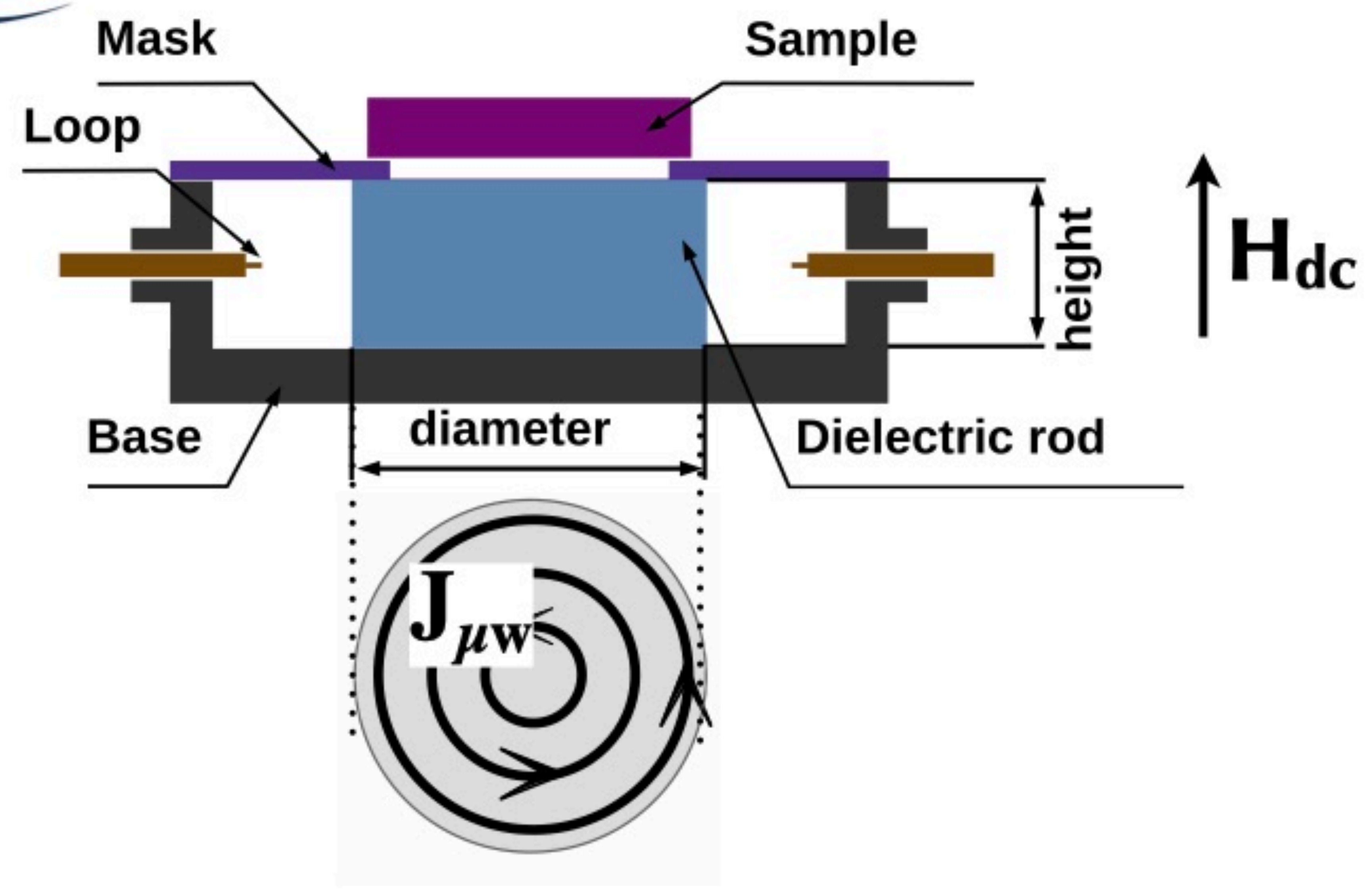


$\mu_0 H \leq 12$ T
$T \geq 4$ K

variable angle
(up to 1.2 T)

Dual frequency
14/24 GHz
16/27 GHz

Sapphire loaded resonator

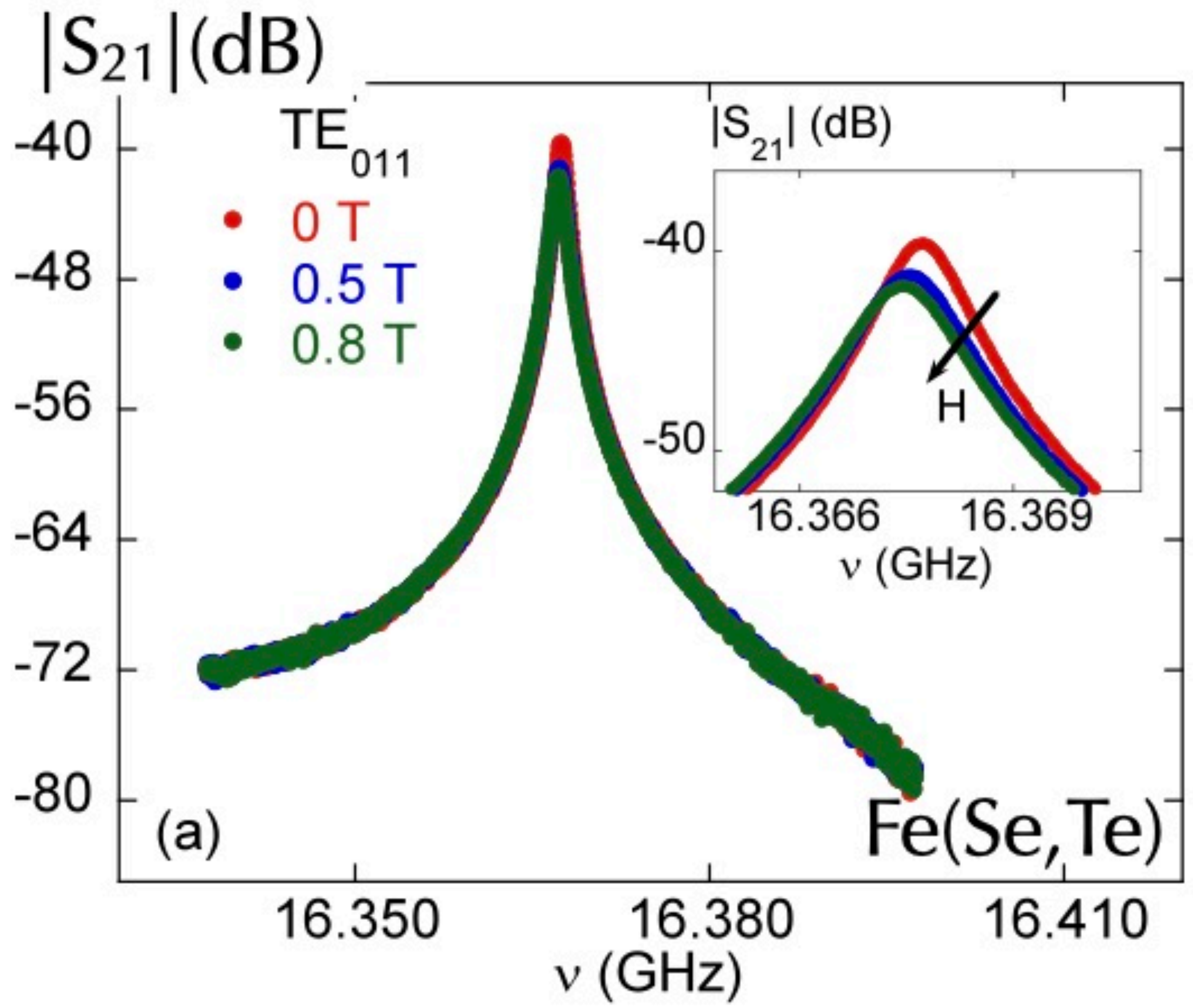


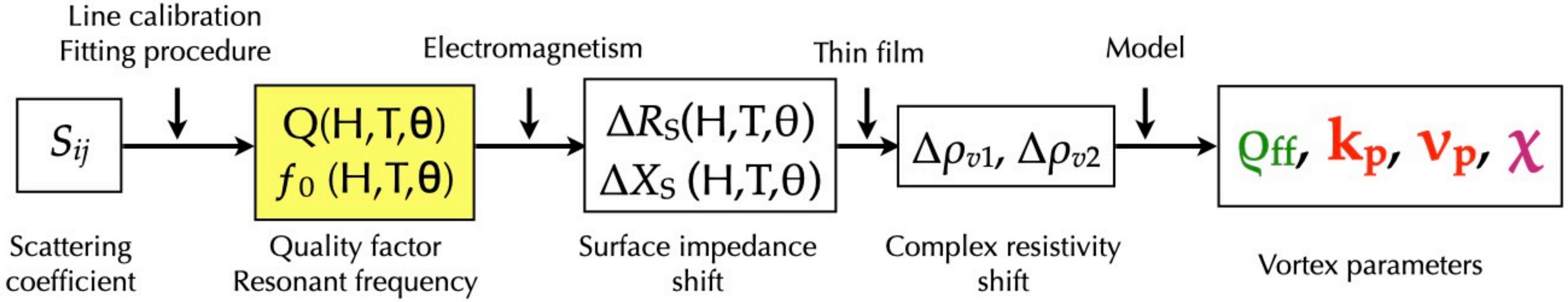


See Pablo Vidal García
Tue, 12:41

K. Torokhtii et al J. Phys.: Conf. Ser. 1065 052027 2018
A. Alimenti et al., Meas. Sci. Technol., 30 065601 2019
N. Pompeo et al., Measurement 184 109937 2021
A. Alimenti et al., IEEE Instrum. Meas. Magazine 24 12 2021

# Microwave technique: data analysis

**Two-mode measurements 16 GHz / 27 GHz, low fields**

**Q-factor and resonance frequency vs. H**

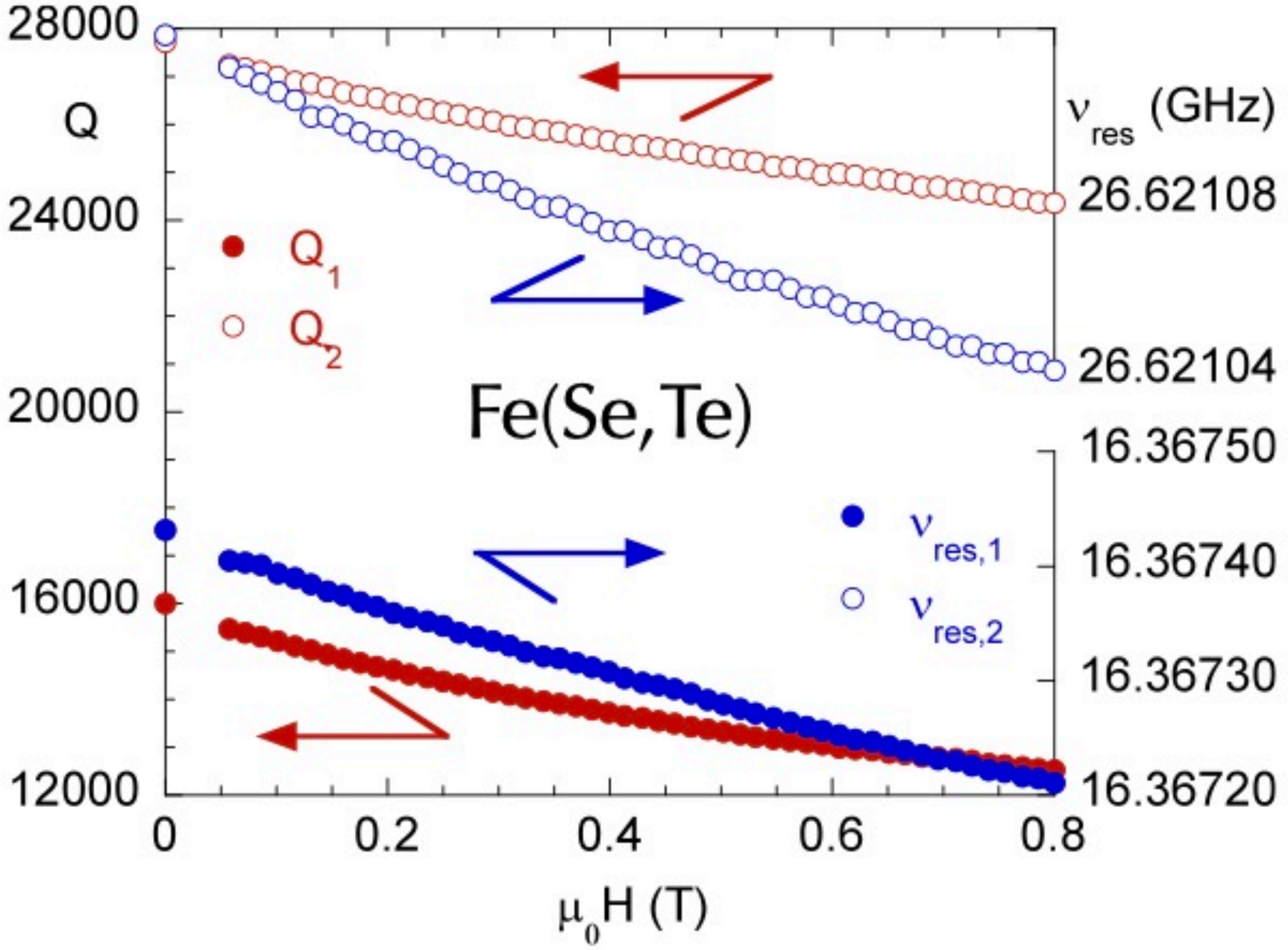


**electromagnetism** → **Surface impedance shift**

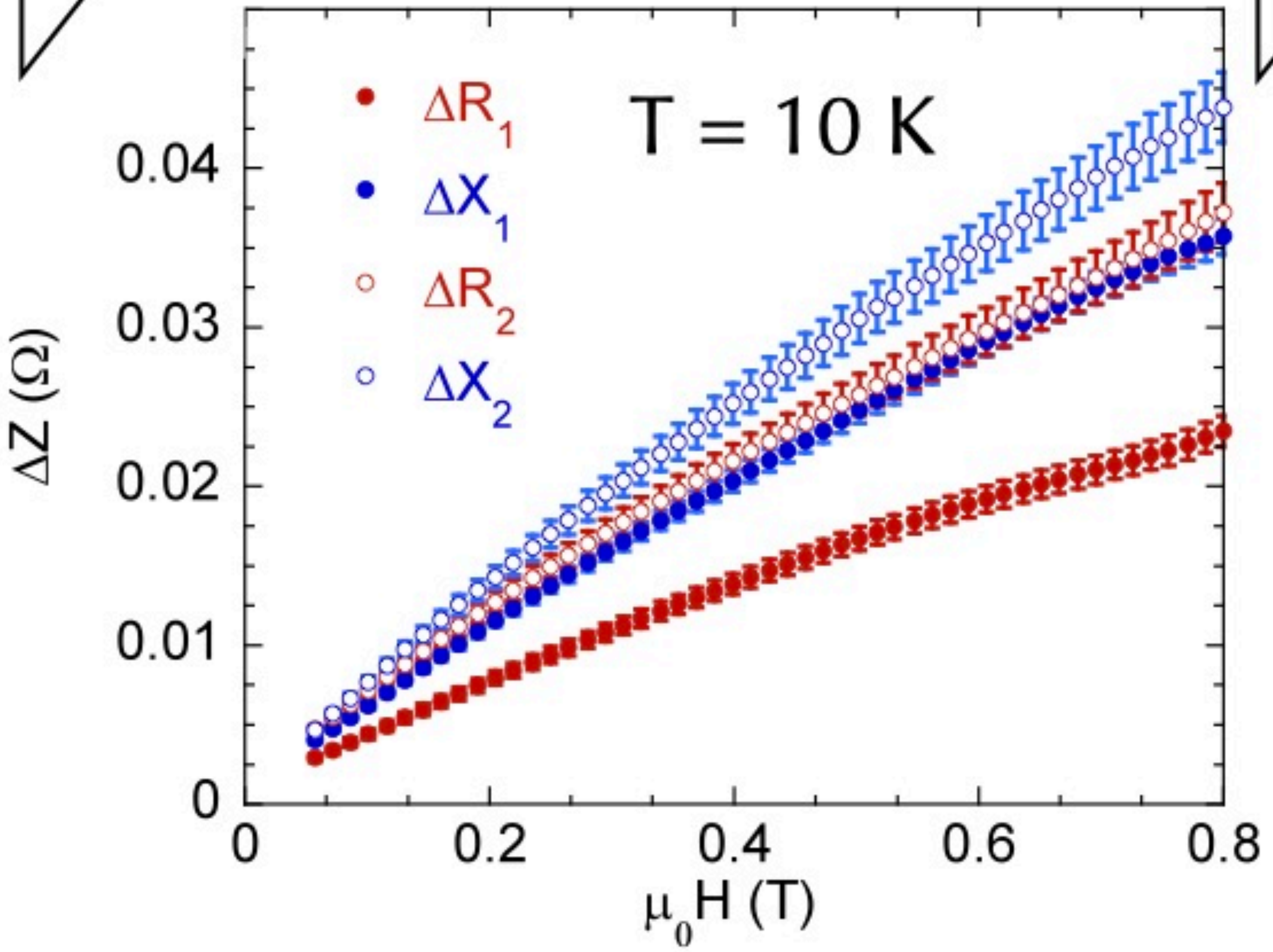


**data inversion** →

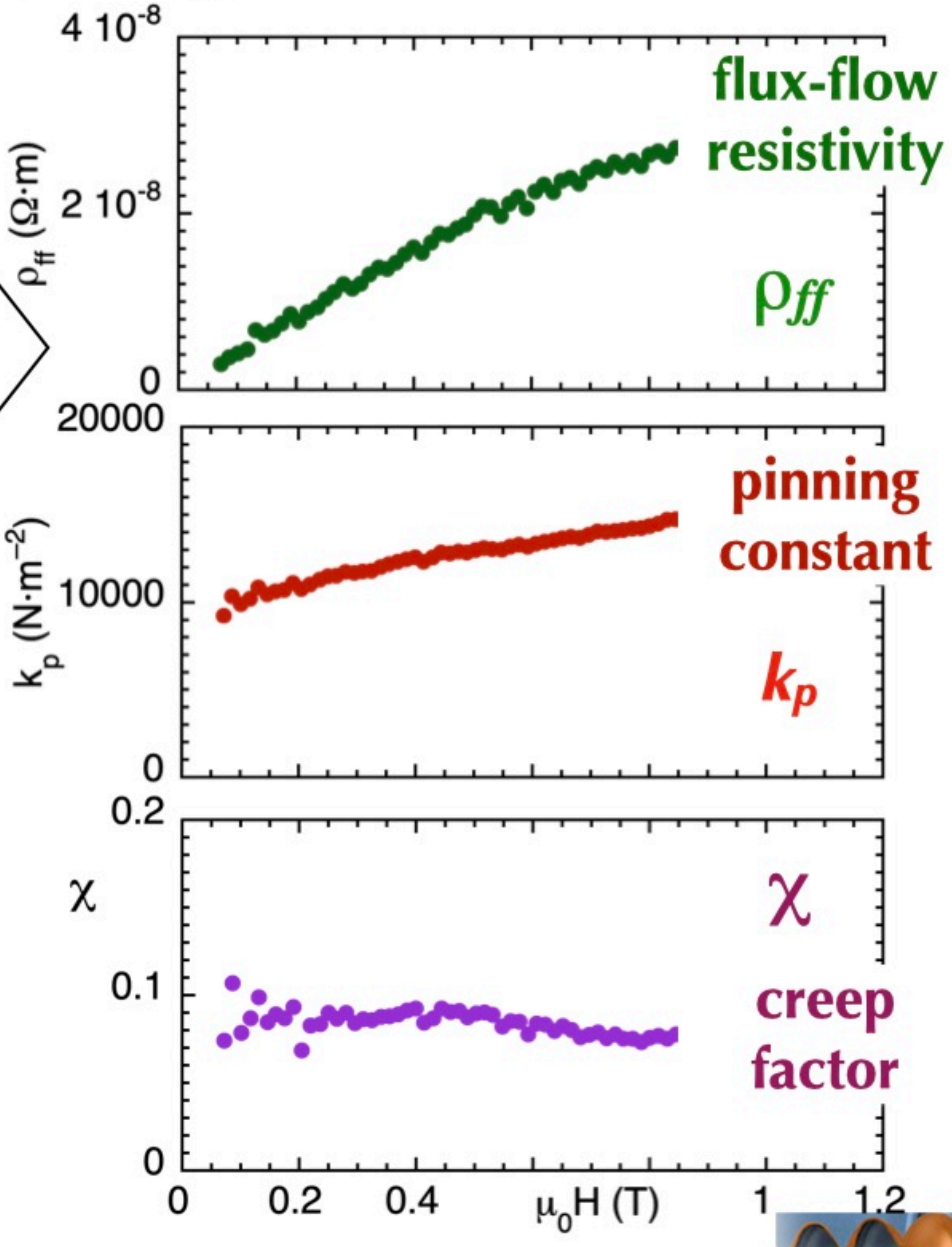


N. Pompeo et al., Measurement 184 109937 2021

# NbTi: a case study

**Measurements in fields**
**$\mu_0 H \leq 1.2$ T**

SAMARA
Superconducting Alternative Materials for Accelerating cavities and haloscope Resonators for Axions

*C. Pira (P.I.)*

# NbTi samples

- $Nb_{40}Ti_{60}$ film (d≃1.70(15) μm) on quartz (1.2 mm)

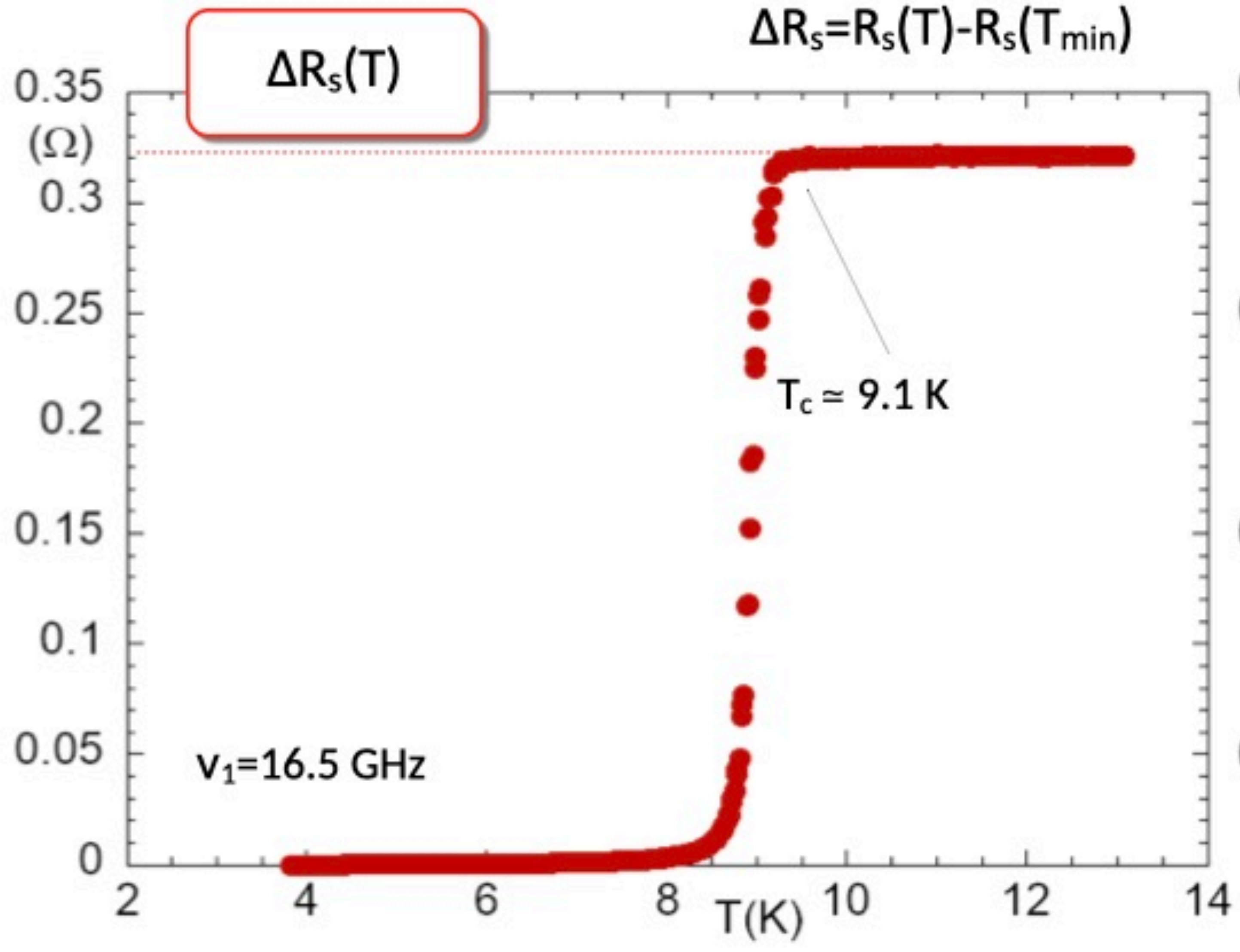


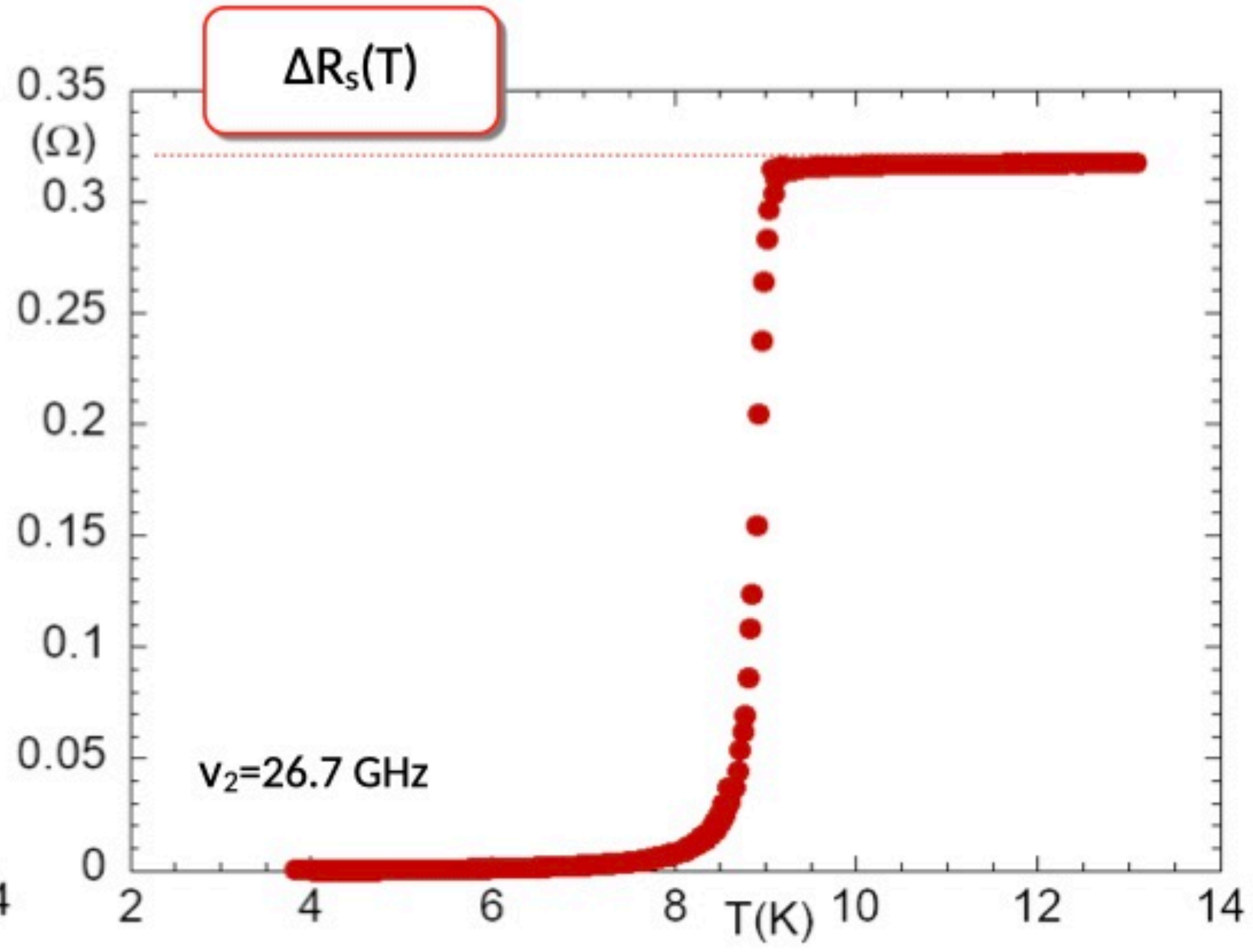


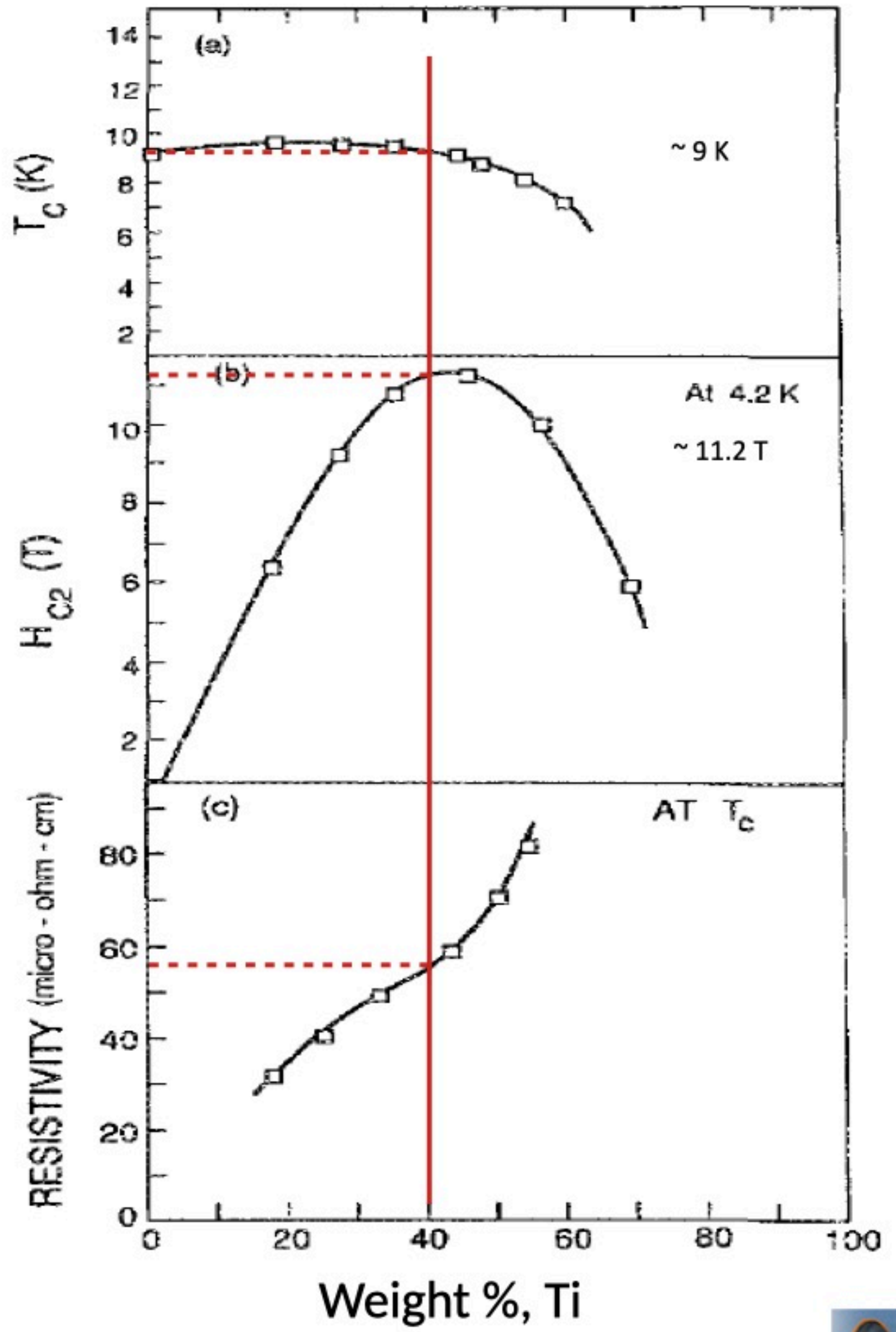


Meingast et al., JAP 66 5962 (1989)

- Normal state resistivity:

$$\rho_n = R_s(T > T_c) \cdot d \simeq 5.4(5) \cdot 10^{-7} \Omega \mathrm{m}$$

$\delta_n \geq 2.9\ \mu m$ ⇒ thin film regime in the normal state

| | $T_c$ [K] | λ [Å] |
|---|---|---|
| $Nb_{0.40}Ti_{0.60}$ | 9.0 | 3000 |
| $Nb_{0.55}Ti_{0.45}$ | 9.6 | 2300 |

(atomic %)

Benvenuti et al, 5th Workshop RF Supercond. 1991

SAMARA
Superconducting Alternative Materials for Accelerating cavities and haloscope Resonators for Axions

*C. Pira (P.I.)*

# NbTi: shift of the surface impedance

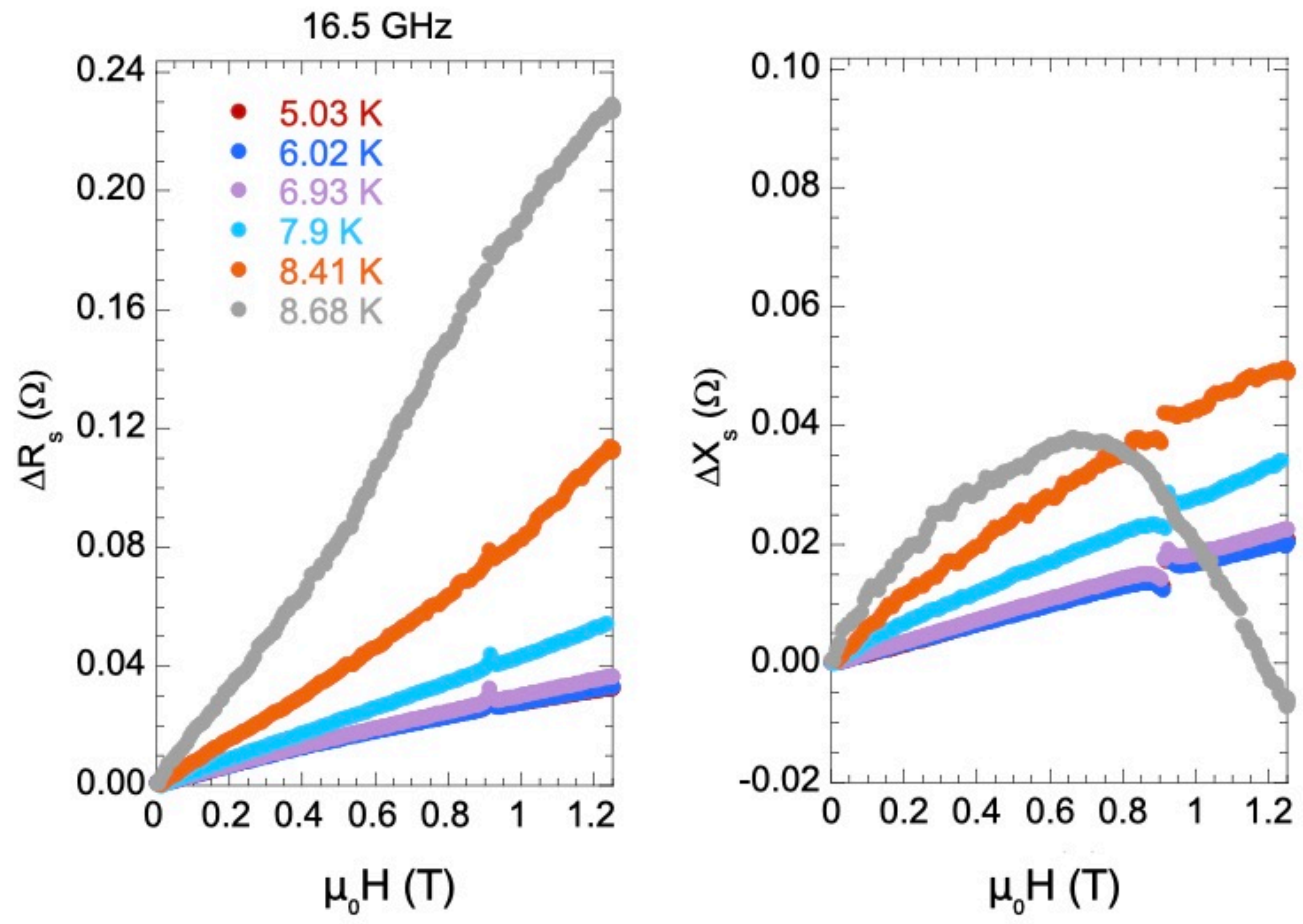


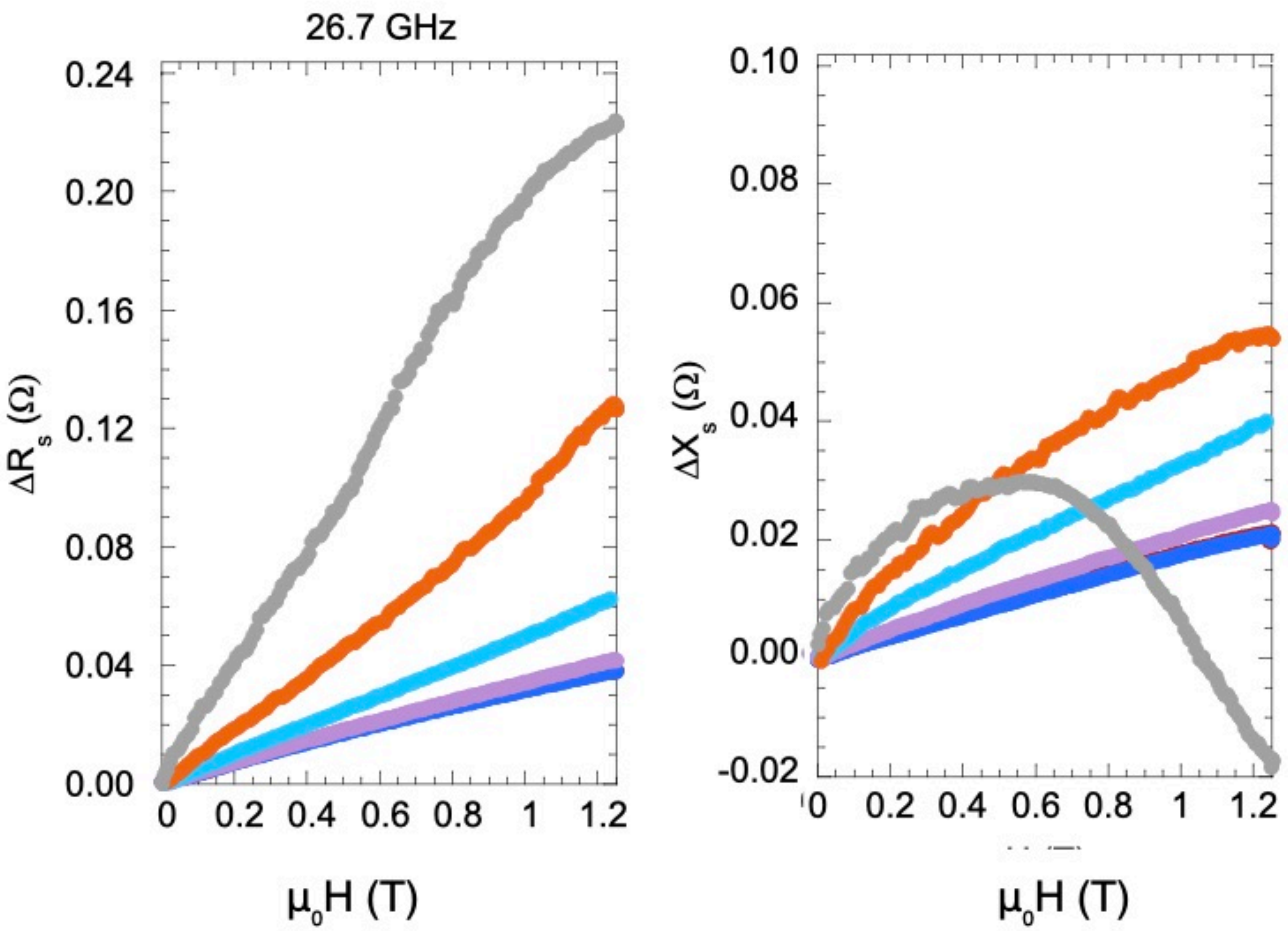


- All T : ΔR & ΔX increase with H
  → vortex motion

- Near $T_c$: large $\Delta R \sim R_n$ & $\Delta X<0$
  → e.m. thin film & 2-fluids contribution

# NbTi: determination of vortex parameters

Simultaneous fits of $Z_s(H) - Z_s(0)$

$$Z_s = \sqrt{\mathrm{i}\omega\mu_0\tilde{\rho}} \qquad \tilde{\rho} \simeq \rho_v + \mathrm{i}\frac{1}{\sigma_2}$$

$$\sigma_2 = \frac{1}{\omega\mu_0\lambda^2} \quad \rho_v = \rho_{ff}\frac{1+\mathrm{i}\frac{\nu_0}{\nu}}{1+\left(\frac{\nu_0}{\nu}\right)^2}$$

Fits yield: $\rho_{ff}$

$\nu_0$

$k_p = \nu_0\Phi_0 B/\rho_{ff}$

at each *H* and *T*

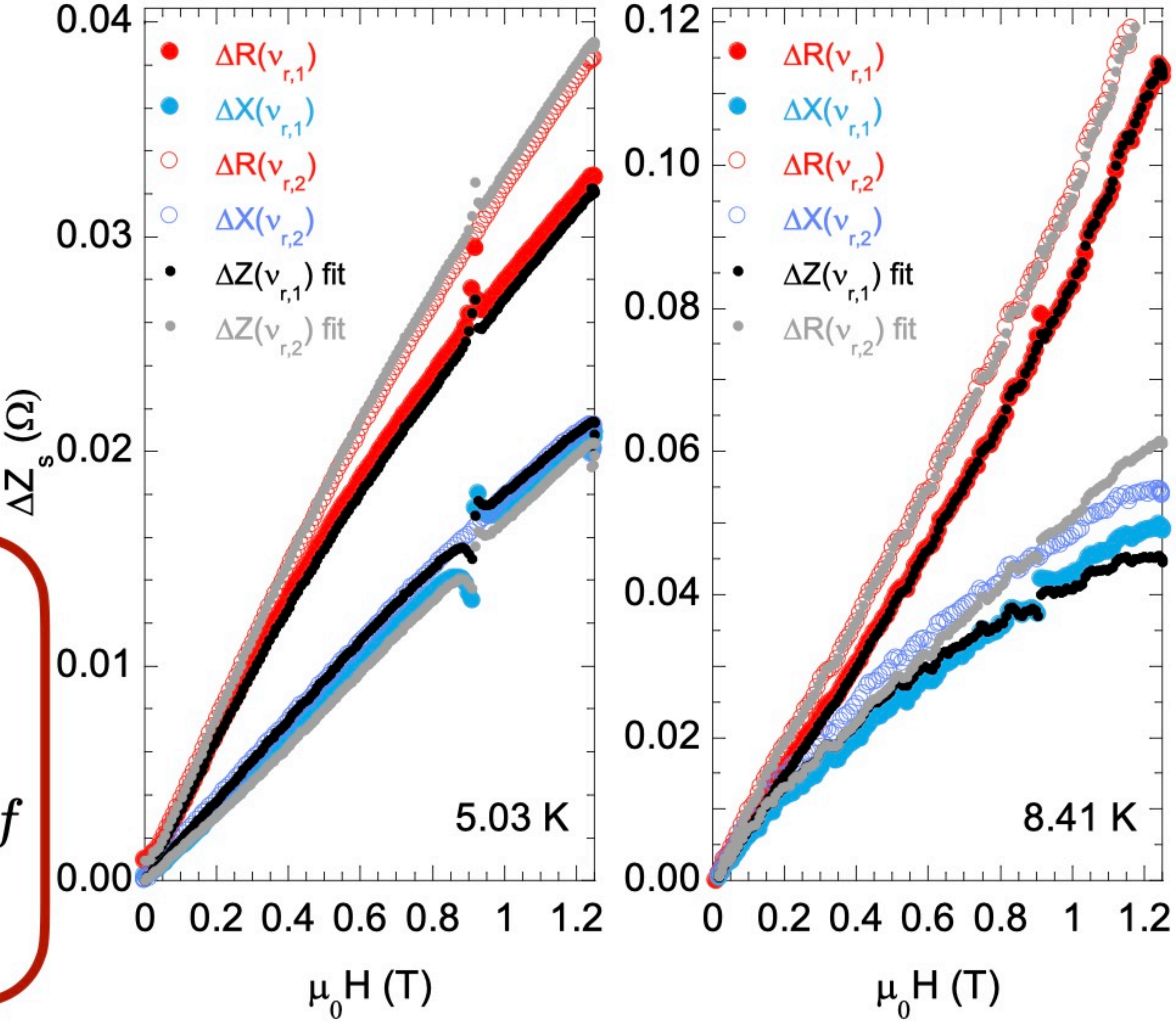

# NbTi: Flux-flow resistivity

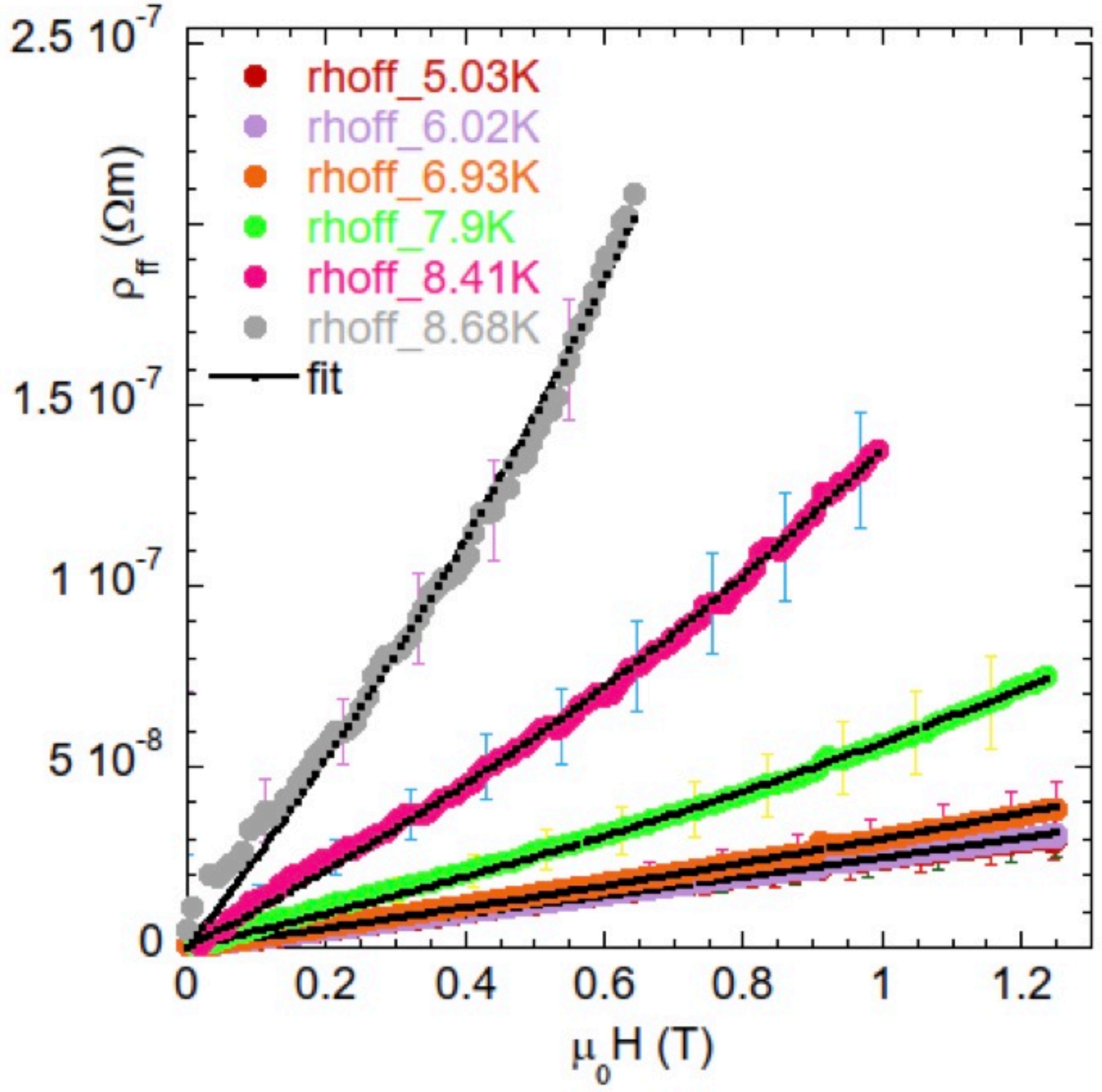


TDGL fits: excellent agreement

$$\rho_{ff} = \rho_n \frac{\alpha B}{(\alpha - 1)B + B_{c2}}$$

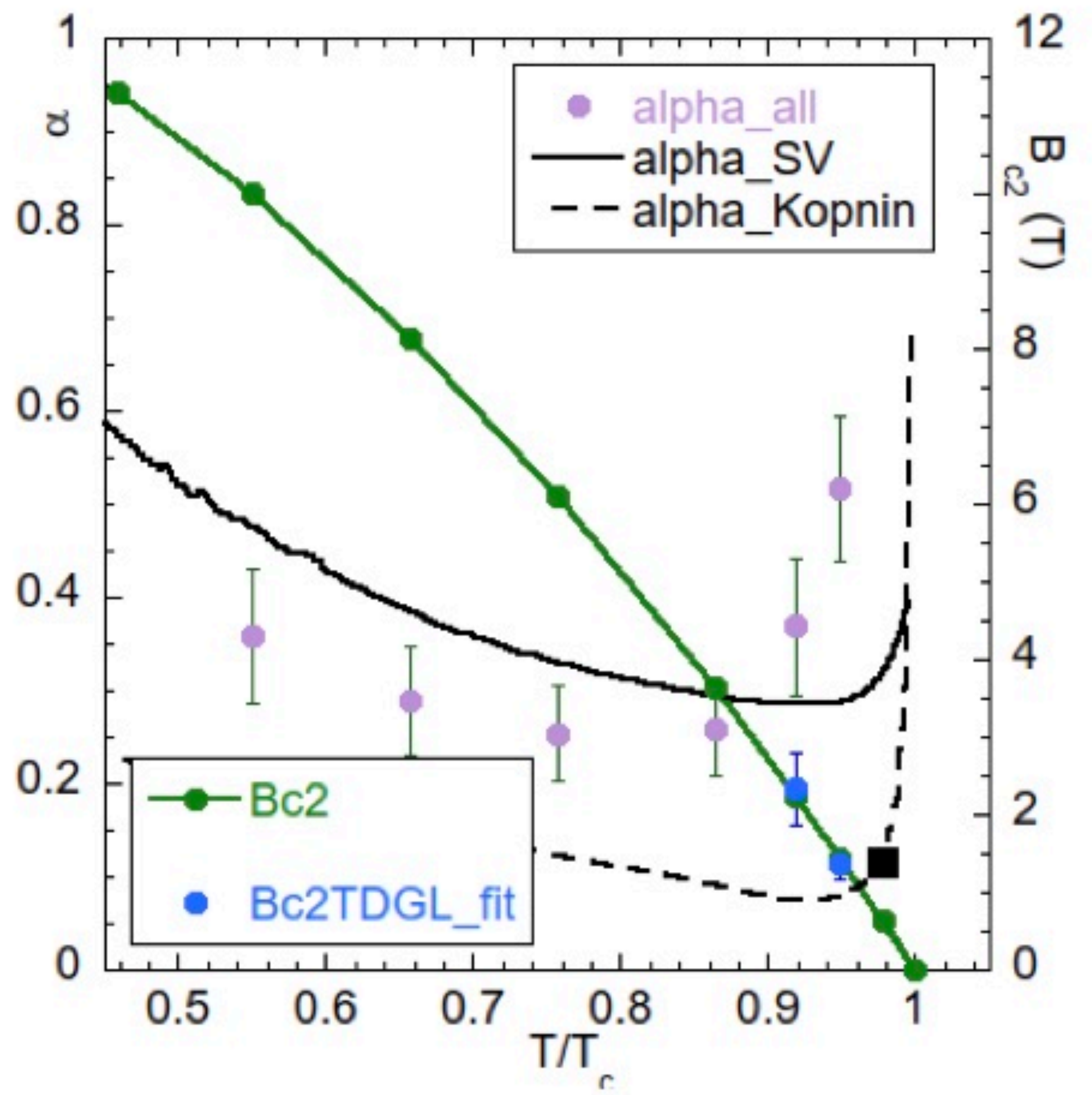

# NbTi: pinning constant (Labusch parameter)

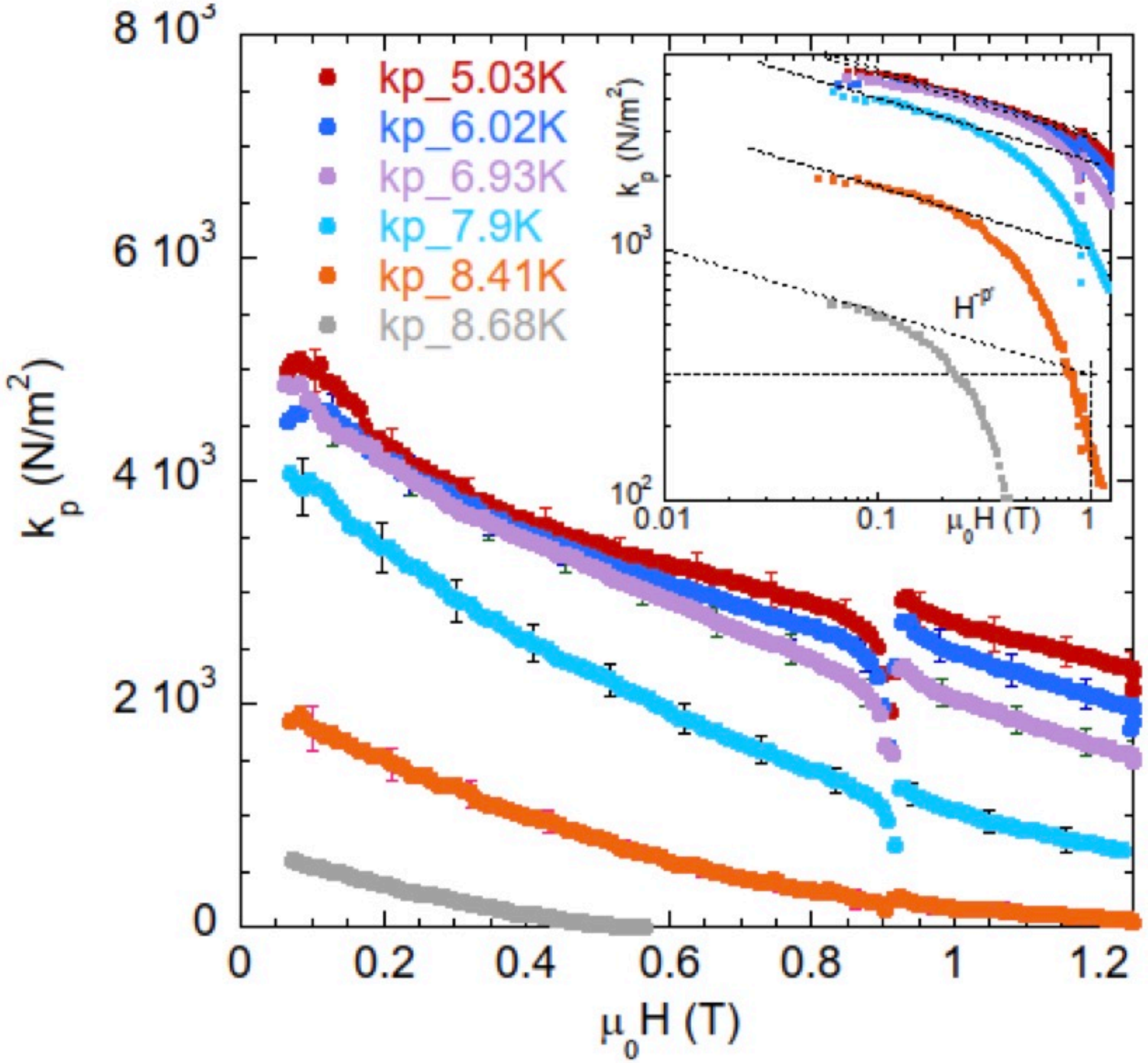


$k_p$ decreases with H
→ depends on fluxon density
→ fluxons are NOT individually pinned by defects
→ collective pinning regime

What are the effective pinning centers?

# NbTi: Dew-Hughes pinning analysis

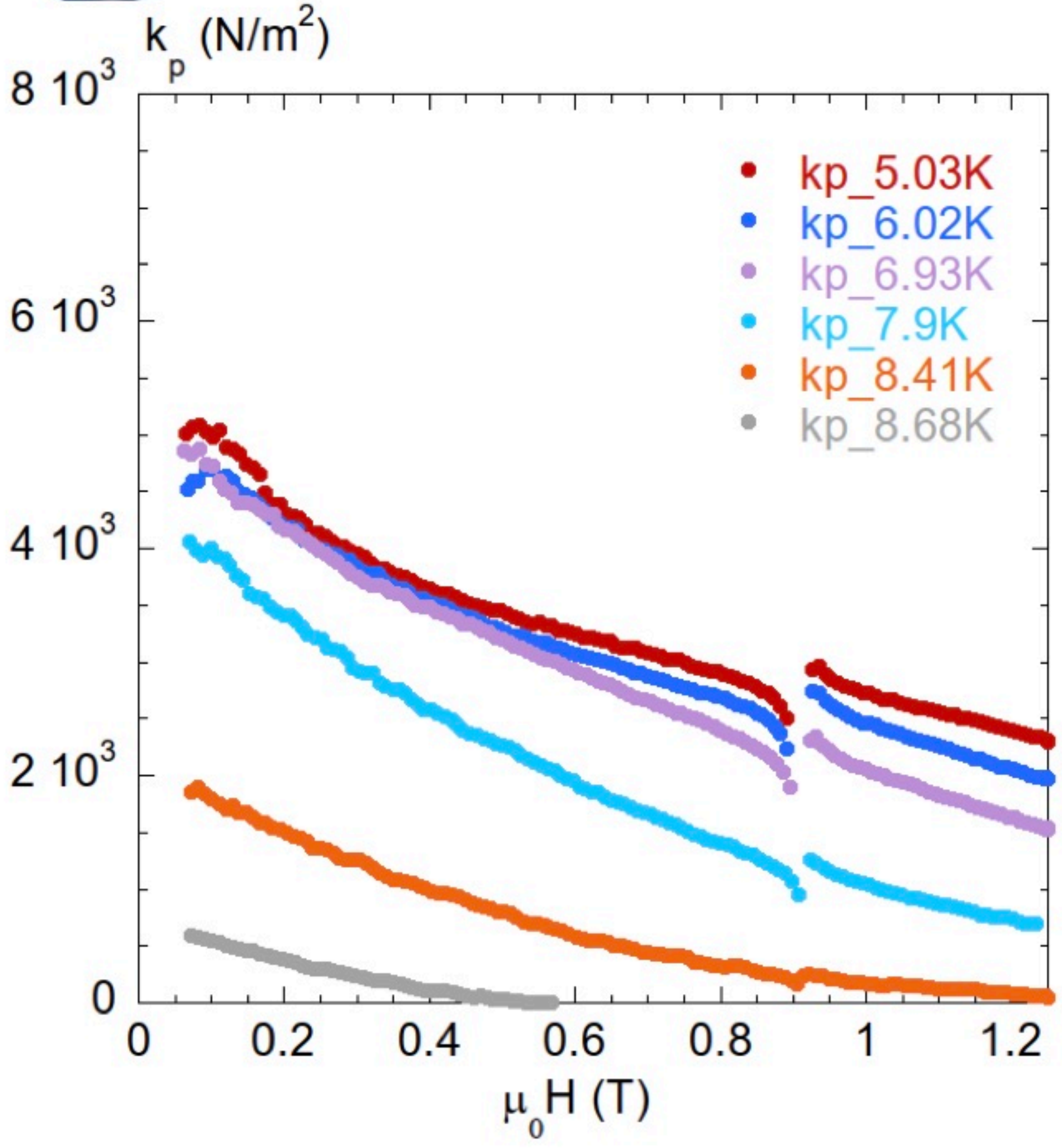


$$F_p(T,B) = \frac{k_p(T,B)\xi(T)B}{\Phi_0}$$

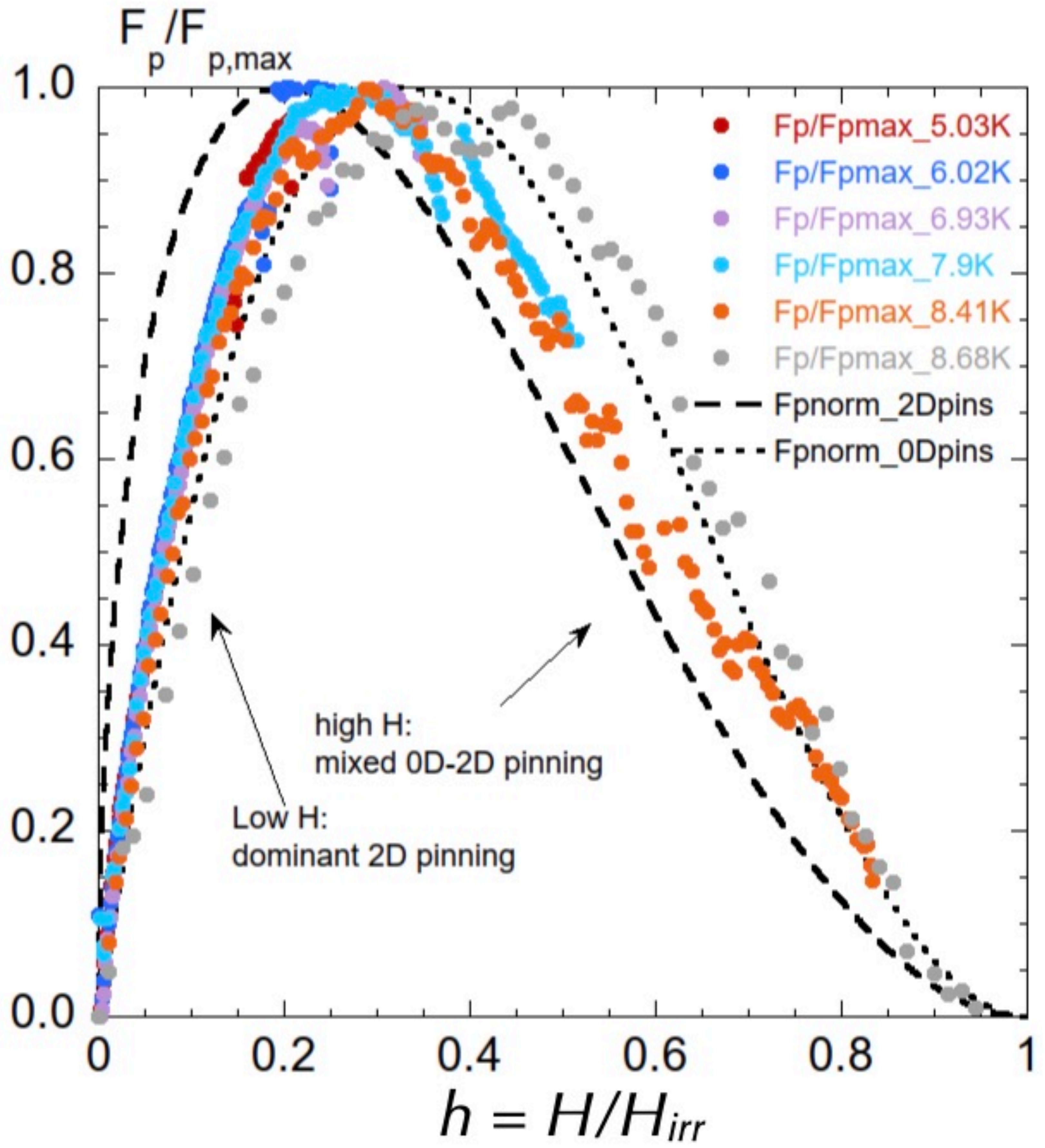


Dew-Hughes scaling analysis: $F_p/F_{p,max} = A \cdot h^p(1-h)^q$

D. Dew-Hughes, Philos. Mag. A J. Theor. Exp. Appl. Phys. 30, 293 (1974).

# NbTi: Dew-Hughes pinning analysis

- data satisfactorily scale with a reduced field $H_{irr} \sim 0.6\ H_{c2}$
- Theory: $q = 2$; $p = 0.5$ (2D pinning), $p = 1$ (0D pinning)

- Result: $q = 2$; $p = 0.75$

⇒ admixture of point (0D) and grain boundary (2D) pinning

- **point pinning dominates at low fields**
- **grain boundaries dominate at high fields**

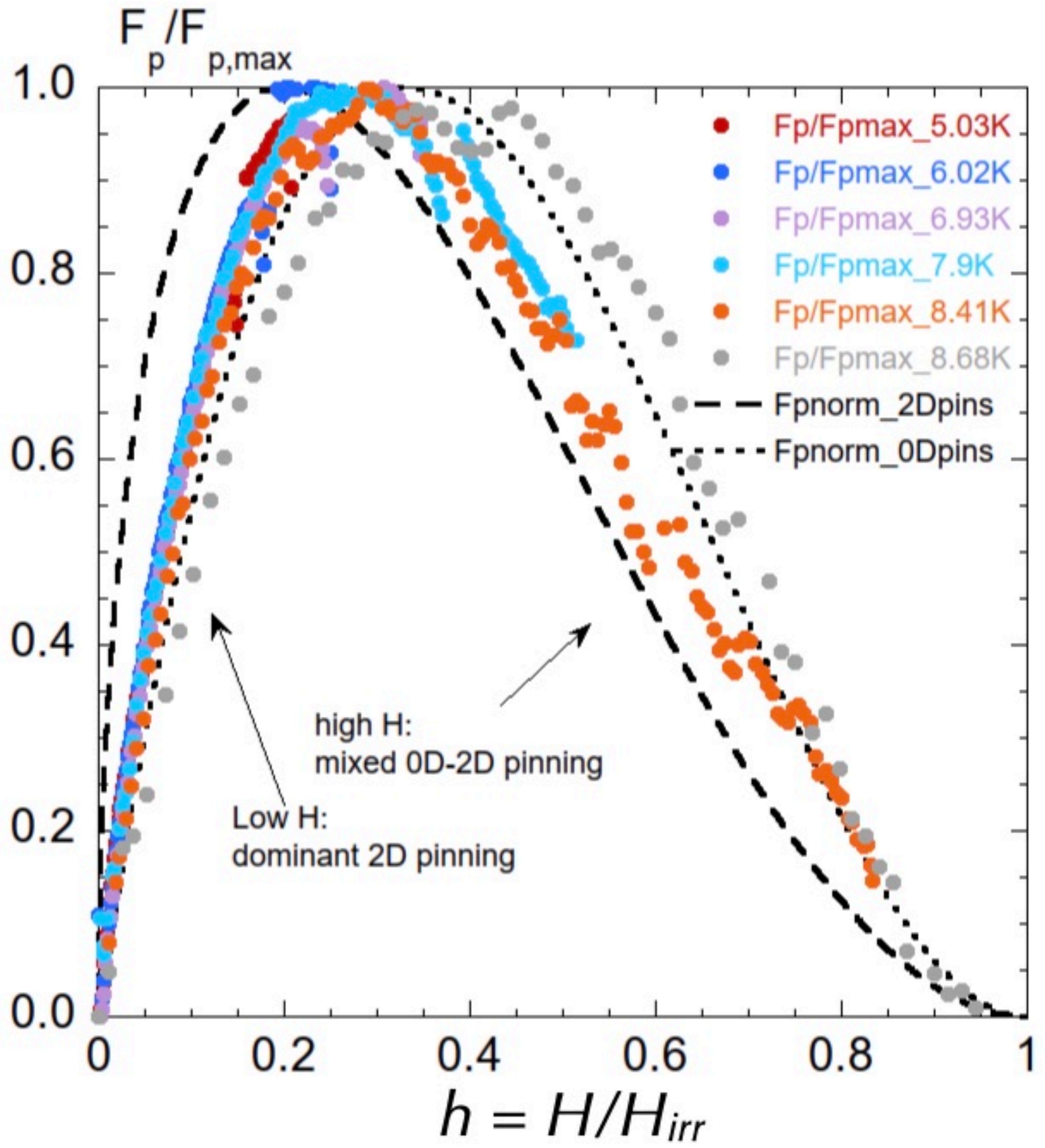


Dew-Hughes scaling analysis: $F_p/F_{p,max} = A \cdot h^p (1-h)^q$

D. Dew-Hughes, Philos. Mag. A J. Theor. Exp. Appl. Phys. 30, 293 (1974).

# Comparison: Fe(Se,Te), YBaCuO

**Measurements in fields**
**$\mu_0 H \leq 12$ T**

# Fe(Se,Te) films – microstructure

$FeSe_{0.5}Te_{0.5}$ Thin film (PLD) on $CaF_2$

$T_c$ = 18 K

thickness $d$ ~ 240 nm

$\varrho_n = 3.0(2) \times 10^{-6}\ \Omega m$

$T_{onset} - T_{zero} = 0.6$ K

RRR=1.1

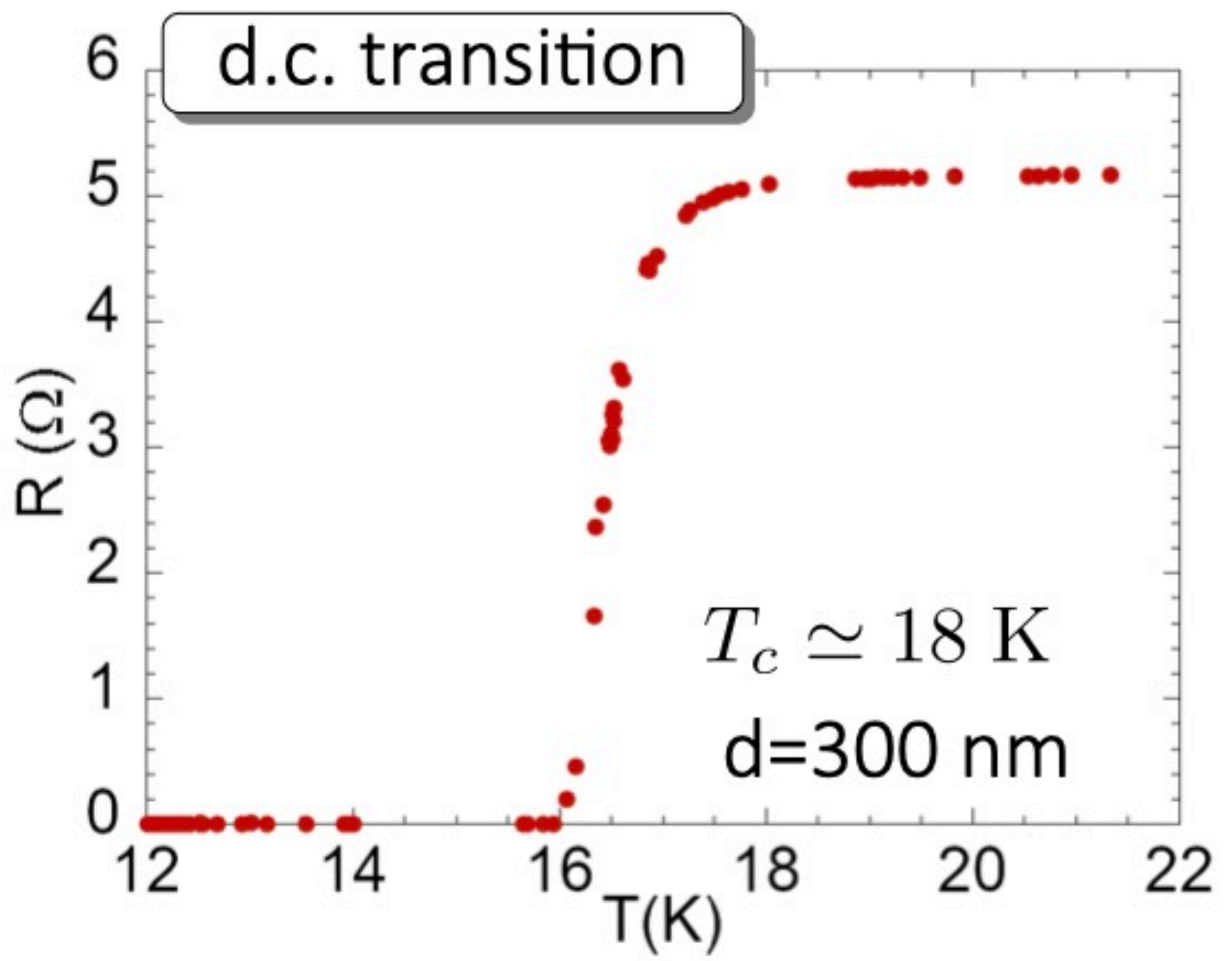


STEM, EELS, HRSTEM

complex pinning landscape most likely

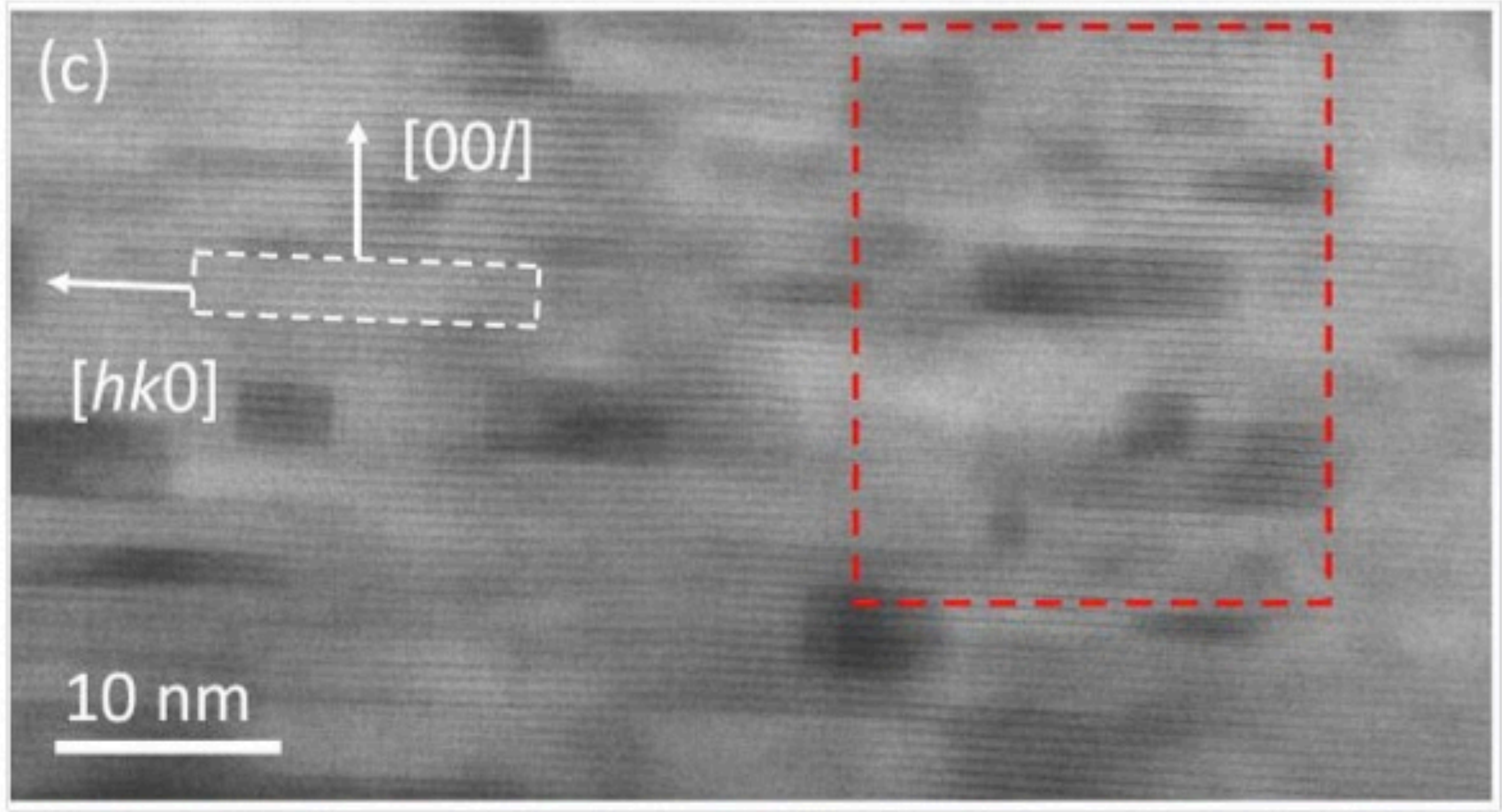


In-plane rotated grains

EELS: Clusters with different stoichiometry (different $T_c$)

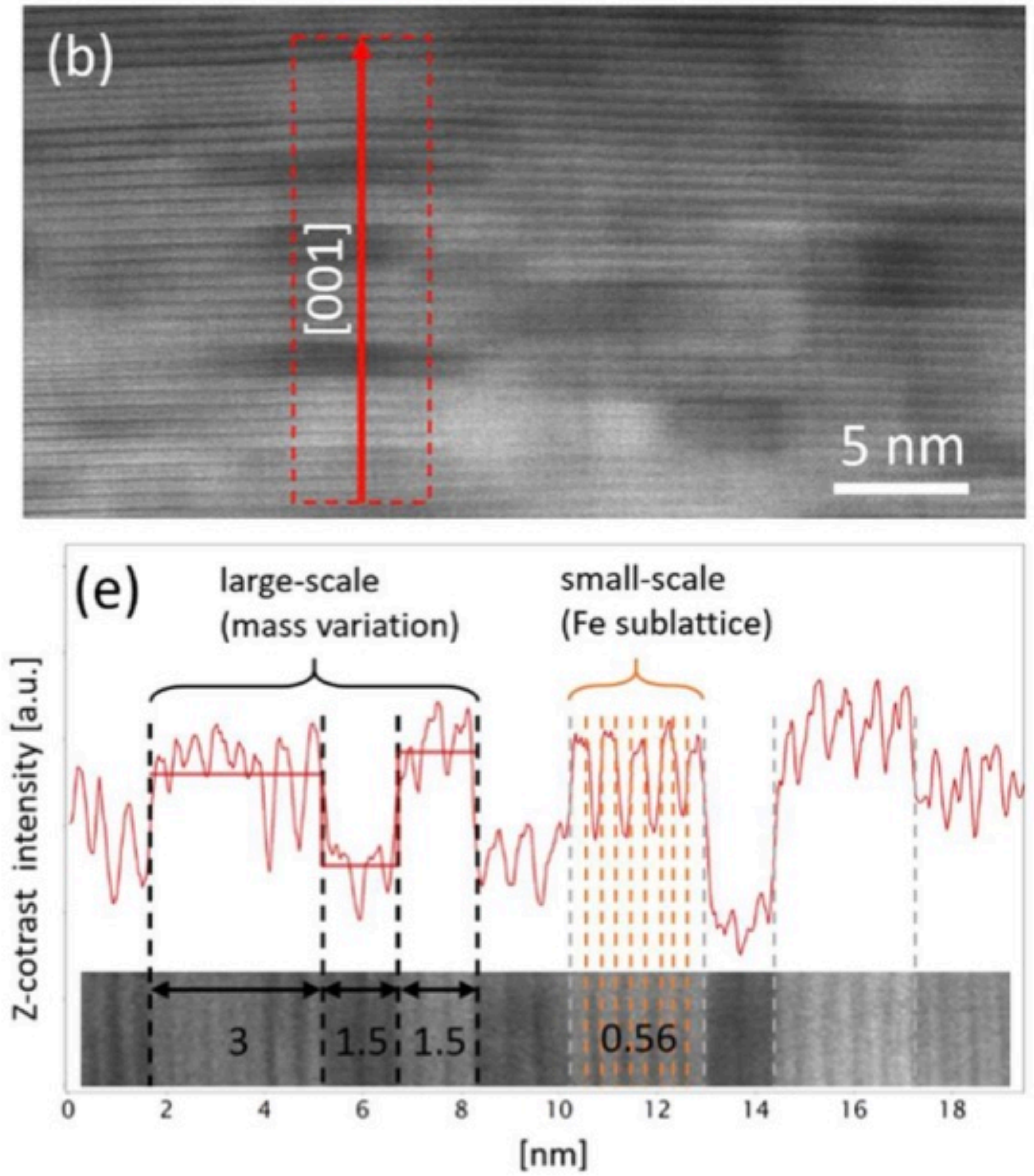


Figure 3. b) STEM Z-contrast image; e) Z-contrast intensity profile along the red line marked in (b).

A. Palenzona et al., SuST 25 115018 2012
V. Braccini et al., APL 103 172601 2013

M. Scuderi et al., Sci. Rep. (2021)

Masood Rauf Khan et al., Materials (2021)

# Fe(Se,Te): Dew-Hughes pinning analysis

**Pinning in Fe(Se,Te) is firmly due to point pinning**

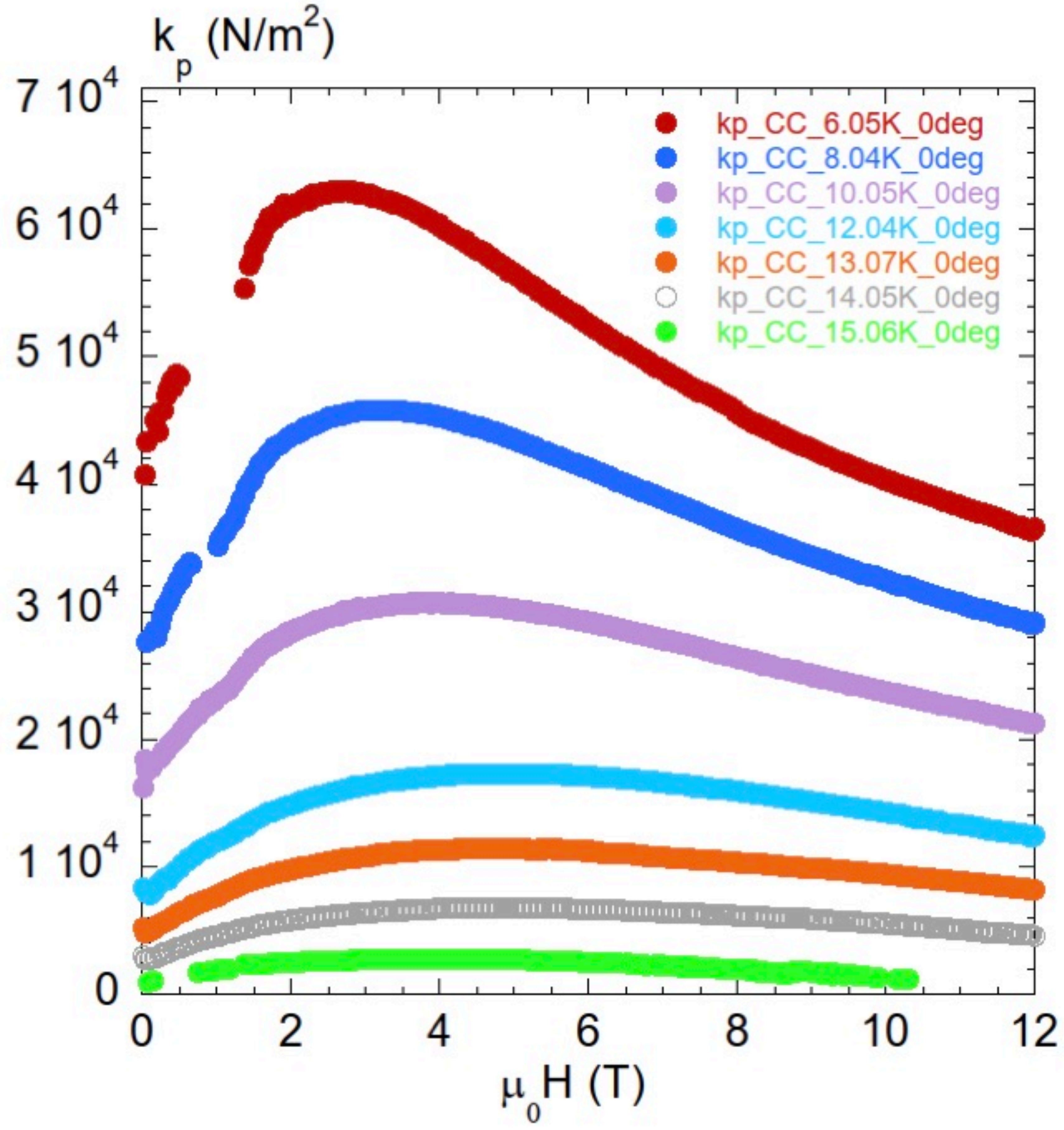


$$F_p(T, B) = \frac{k_p(T, B)\xi(T)B}{\Phi_0}$$

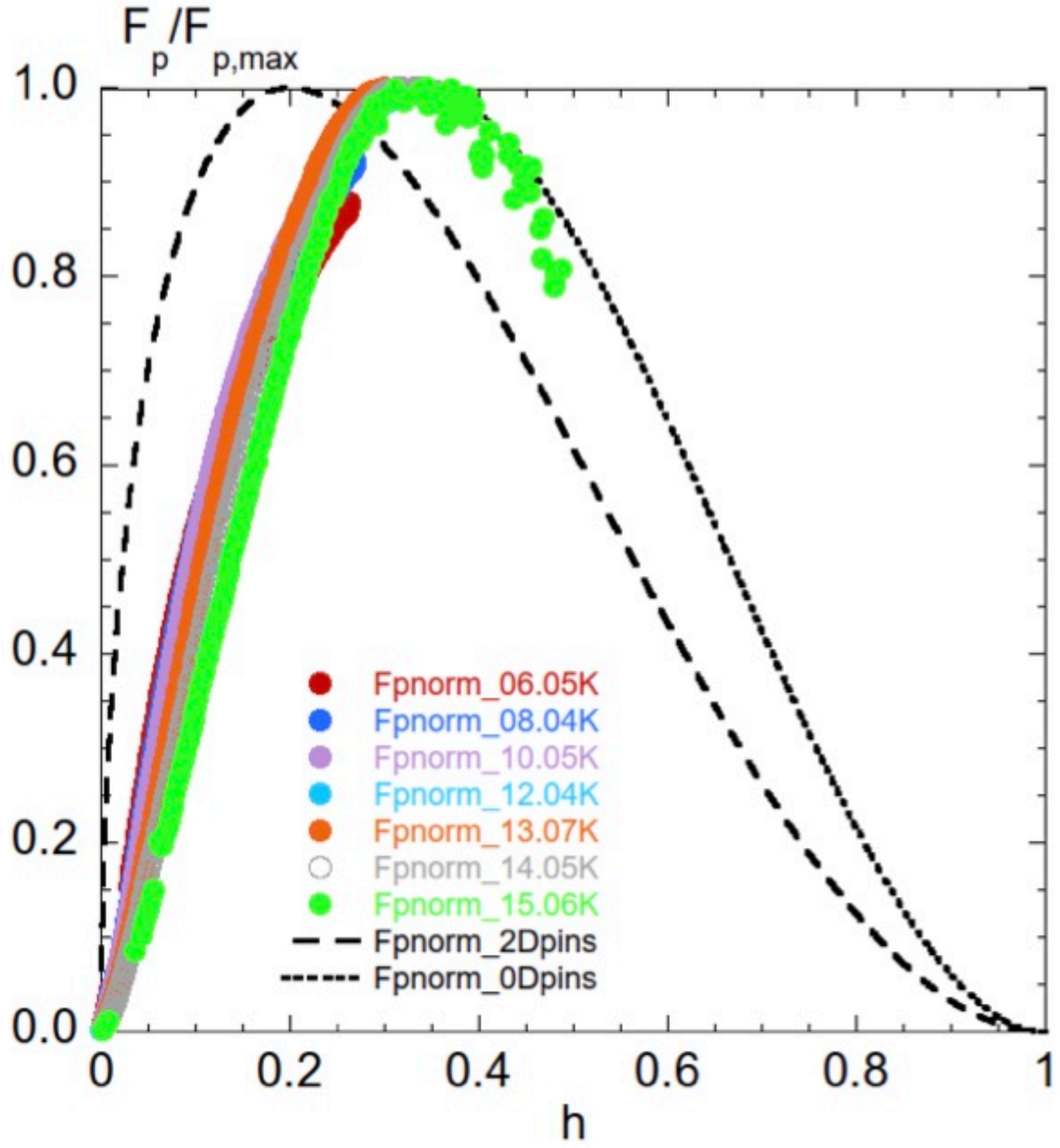


Dew-Hughes scaling analysis: $F_p/F_{p,max} = A \cdot h^p(1-h)^q$

D. Dew-Hughes, Philos. Mag. A J. Theor. Exp. Appl. Phys. 30, 293 (1974).

# YBaCuO: single pinning regime

**Pinning in YBaCuO: single vortex pinning.**
**Impossible to determine whether 0D, 2D pinning**

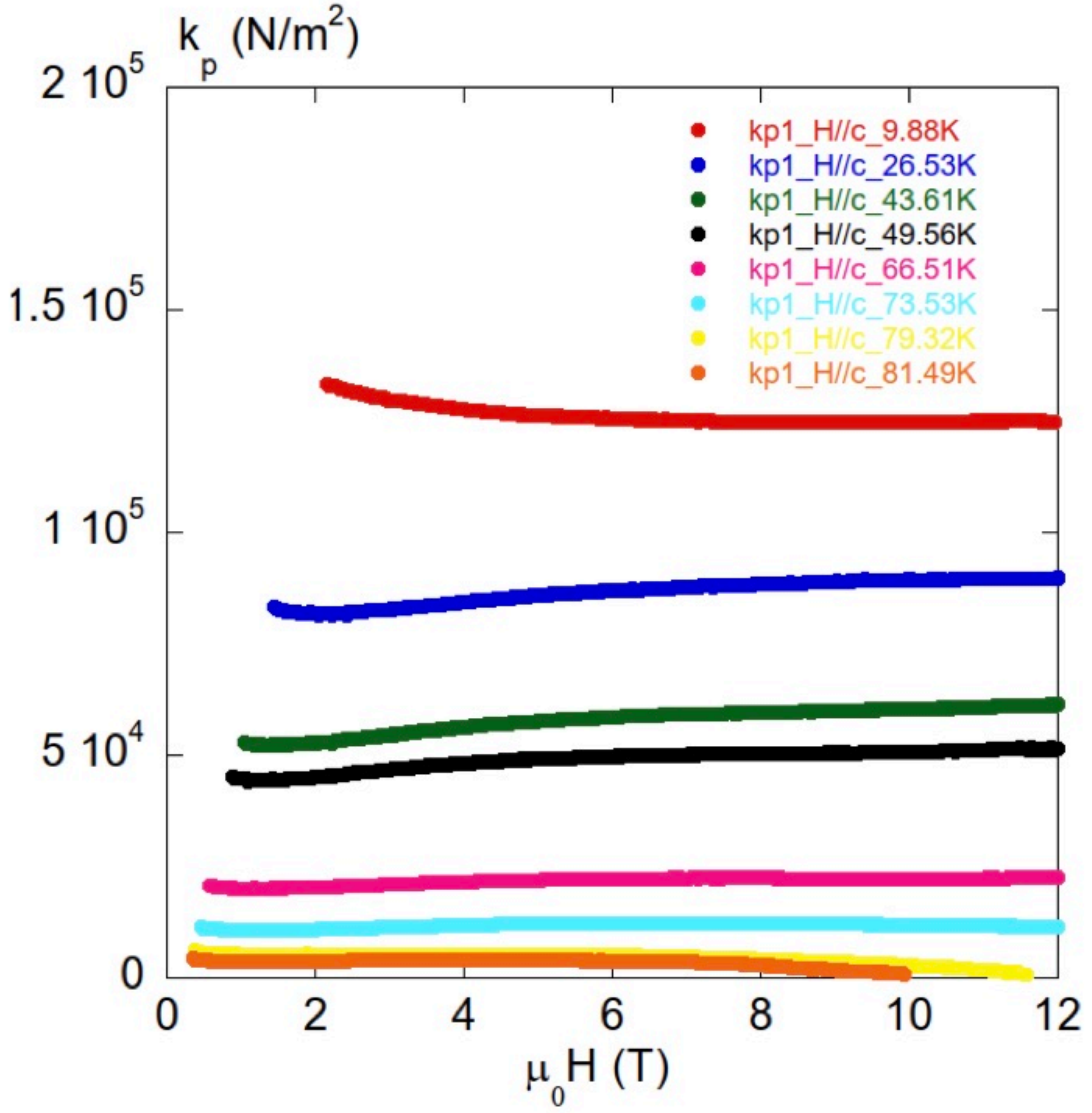


Sample details: V. Pinto et al., Coatings, vol. 10, no. 9, art. id. 860, 2020.
YBCO pristine,
CSD growth
Substrate: LAO
Thickness: 80 nm
Tc(0)= 89.86 K

## Reexamination of NbTi haloscope data: experimental estimate of $c_{ff}$

**Combining vortex parameters +**
**$R_s$+i$X_s$ data on an haloscope**

**⇒ experimental determination of the alignment factor $c_{ff}$**

# NbTi: reexamination of haloscope data - procedure

**Vortex parameters: this work**

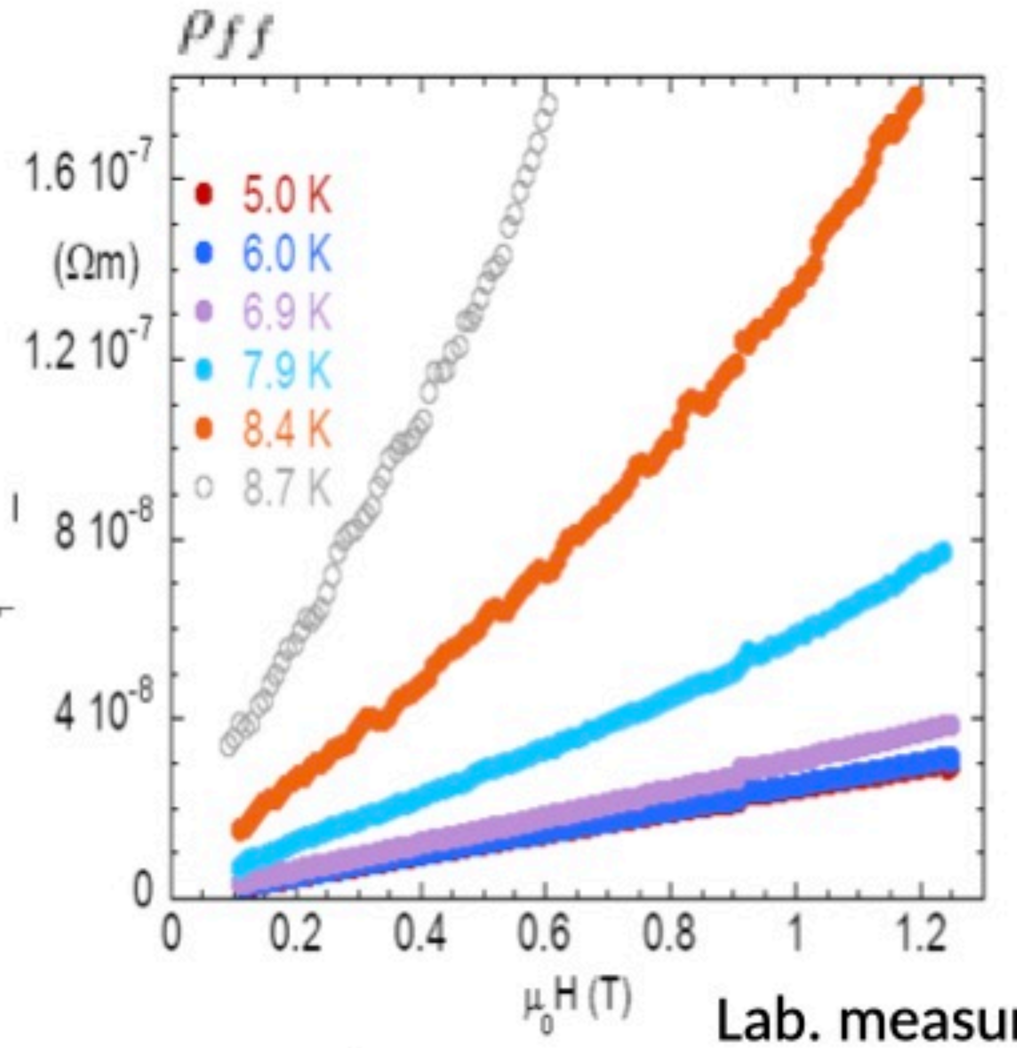


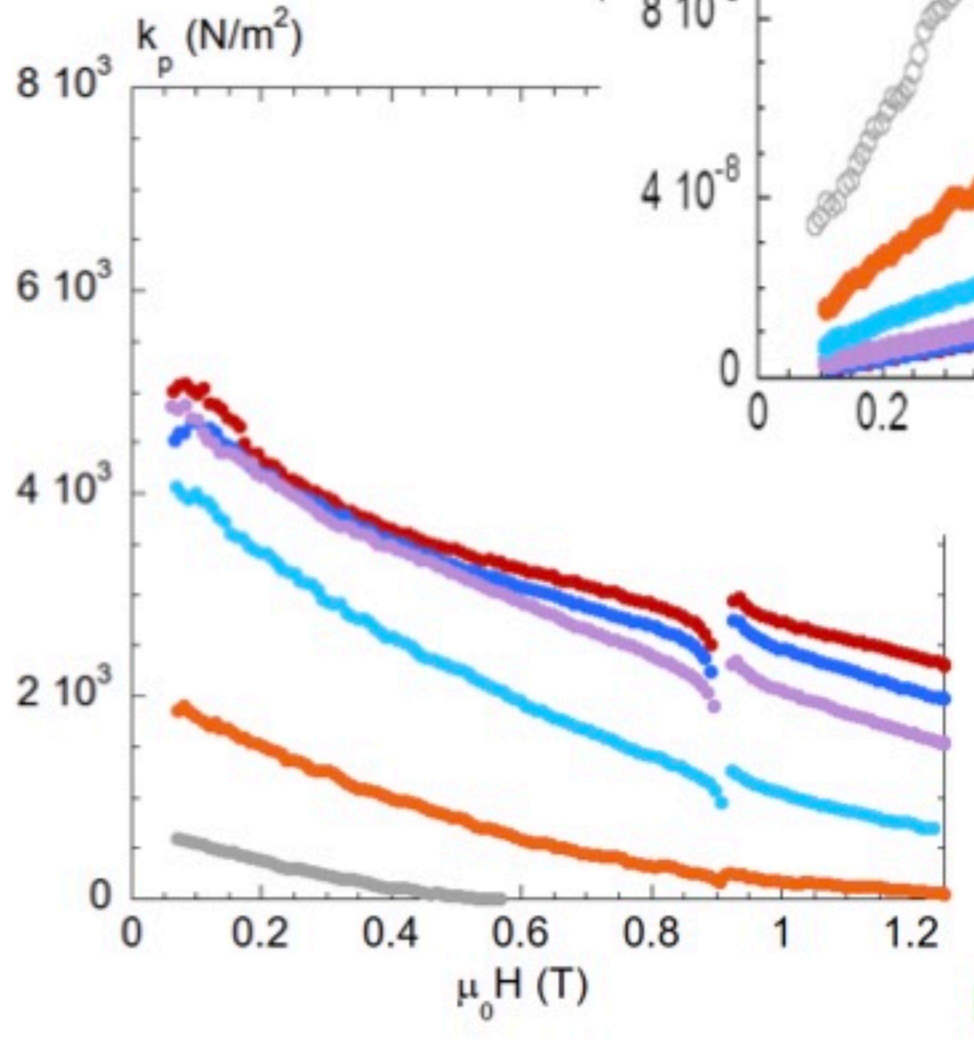


Lab. measurement setup
max. Lorentz force

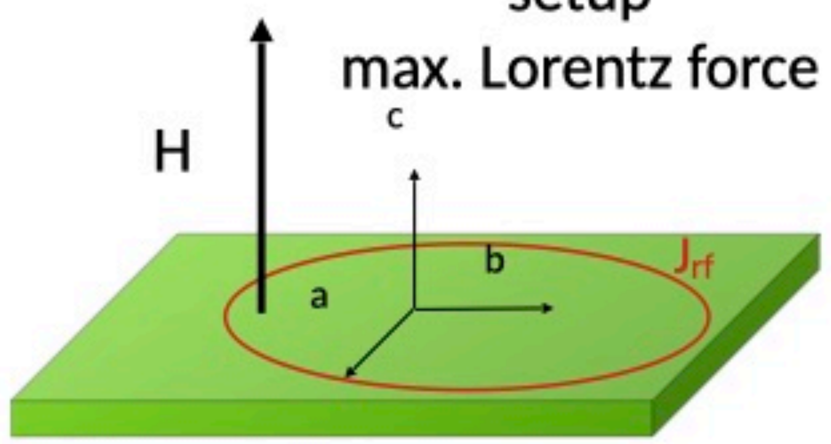


\+

**model**

$$Z_s = \sqrt{\mathrm{i}\frac{\omega\mu_0}{\sigma}} = \sqrt{\mathrm{i}\omega\mu_0\tilde{\rho}}$$

$$\tilde{\rho} = \frac{\rho_v + \mathrm{i}\frac{1}{\sigma_2}}{1 + \mathrm{i}\frac{\sigma_1}{\sigma_2}}$$

$$\sigma_1 - \mathrm{i}\sigma_2 = \frac{n_n e^2 \tau}{m} - \mathrm{i}\frac{1}{\omega\mu_0\lambda^2}$$

$$\rho_v = c_{ff}\ \rho_{ff}\frac{\chi + \mathrm{i}\frac{\nu}{\nu_0}}{1 + \mathrm{i}\frac{\nu}{\nu_0}}$$

⇒

**fit to nominally force-free configuration data with one parameter: $c_{ff}$**

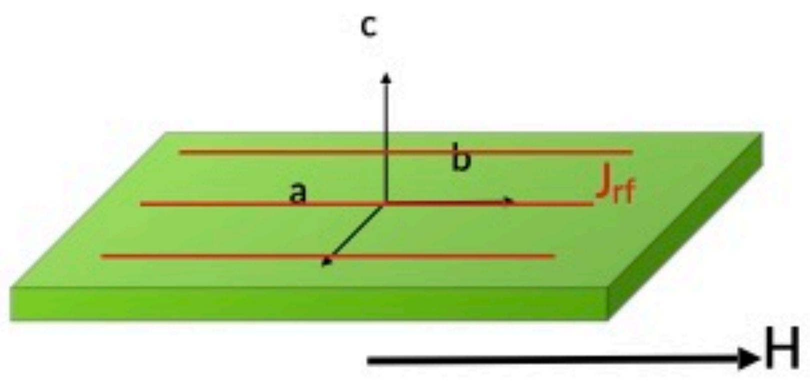


Haloscope
"force free" config.

# NbTi: reexamination of haloscope data - results

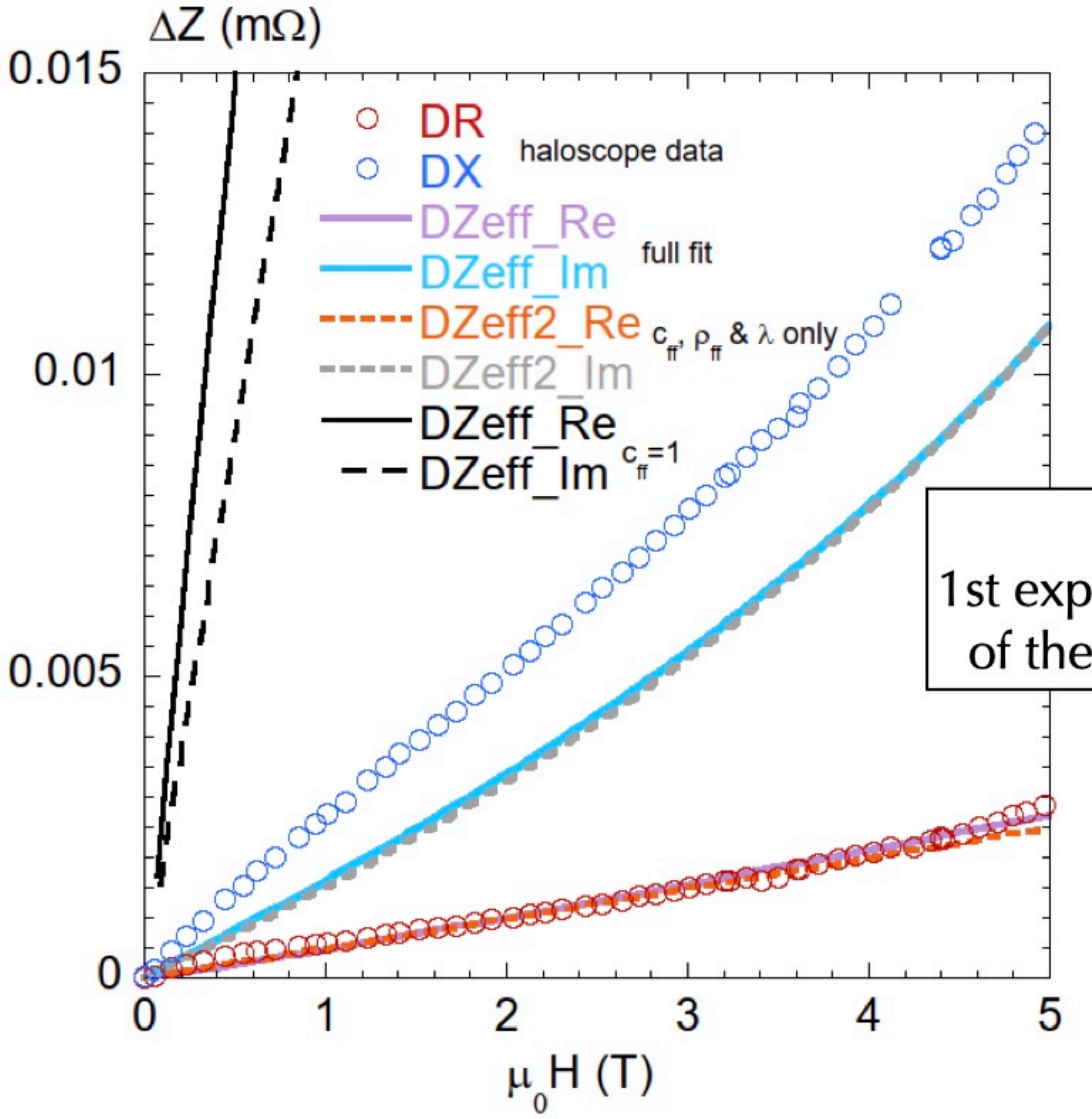


$c_{ff} = 0.012$
1st experimental estimate
of the alignment factor

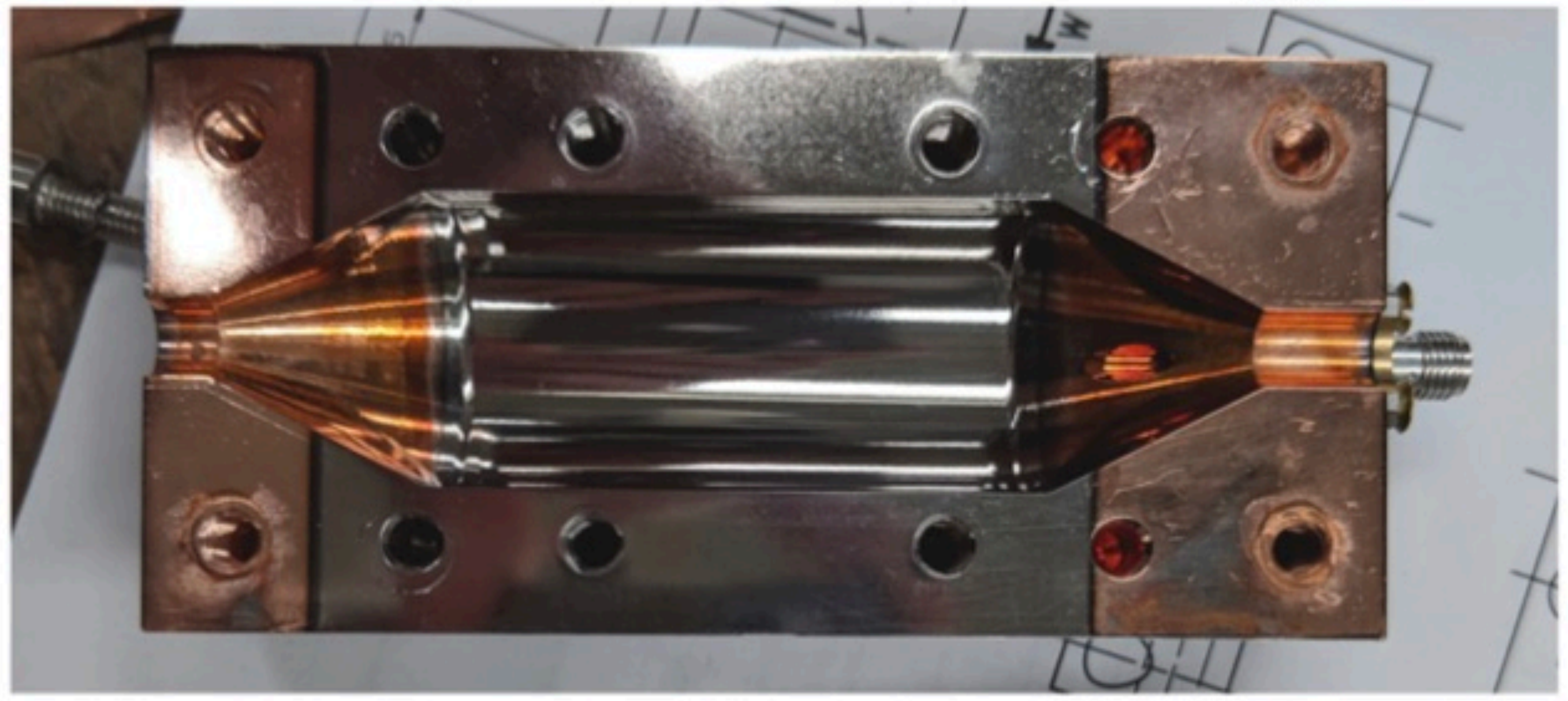

**NbTi haloscope**

Alesini et al.
*Phys. Rev. D* **99** 101101(R) (2019)

**fit to nominally force-free configuration data with one parameter: $c_{ff}$**

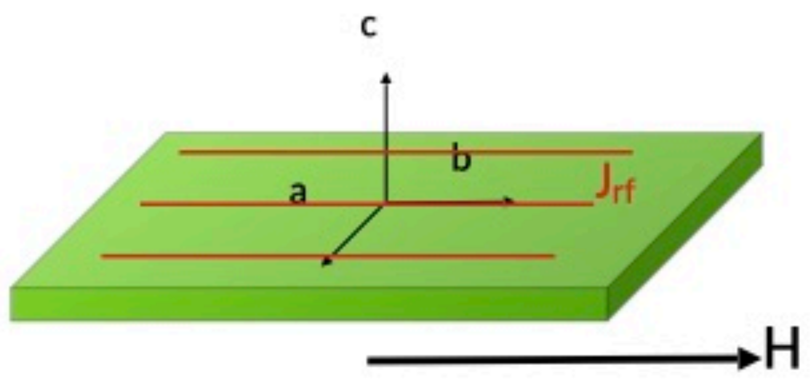


Haloscope
"force free" config.





thinfilms

# Evaluation of the potential for haloscopes

# Comparison of superconductors

$$R_s \simeq \frac{1}{2} c_{ff} \rho_{ff} \frac{1}{1+(\nu_0/\nu)^2} \frac{1}{\lambda}$$

calculated at $B$ = 5 T
T = 4.2 K
$\nu$ = 9 GHz

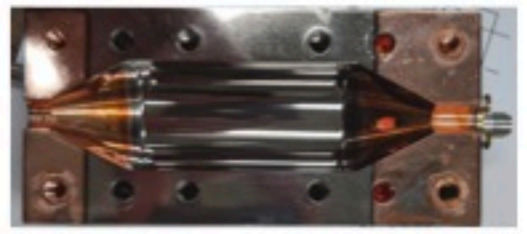

| | NbTi | $Nb_3Sn$ | YBaCuO | Fe(Se,Te) |
|---|---|---|---|---|
| $c_{ff}$ | 0.012 (this work) | 0.011 (calculated) | 0.0042 (calculated) | 0.093 (calculated) |
| $\rho_{ff}$ ($\mu\Omega \cdot$ cm) | 10 | 1.2 | 0.54 | 3.2 |
| $\nu_0$ (GHz) | 1.5 | 1.3 | 59 | 69 |
| $k_p$ ($N \cdot m^{-2}$) | 100 | 7055 | $7.1 \cdot 10^6$ | $1.4 \cdot 10^5$ |
| $\frac{1}{1+(\nu_0/\nu)^2}$ | 0.973 | 0.98 | 0.023 | 0.017 |
| λ (nm) | 300 (literature) | 250 (P. Vidal García, TUE) | 150 (ab, literature) | 540 (ab, literature) |
| $R_s$ (mΩ) | 2.1 | 0.27 | 0.0017 | 0.046 |

# Comparison of superconductors: $R_s$ vs $B$ - haloscope configuration

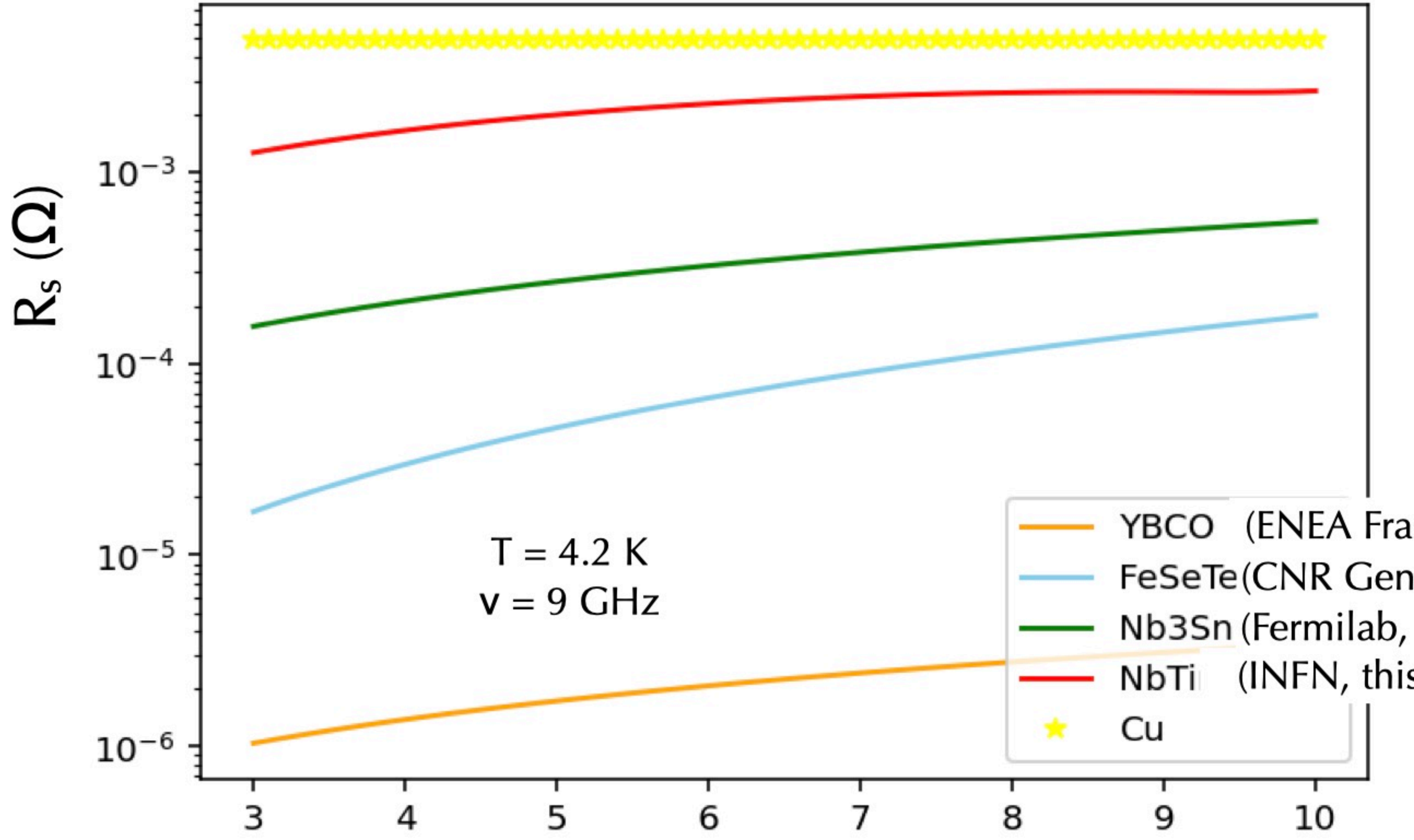


warning:
includes $c_{ff}$ calculated for the cylinder of the INFN haloscope

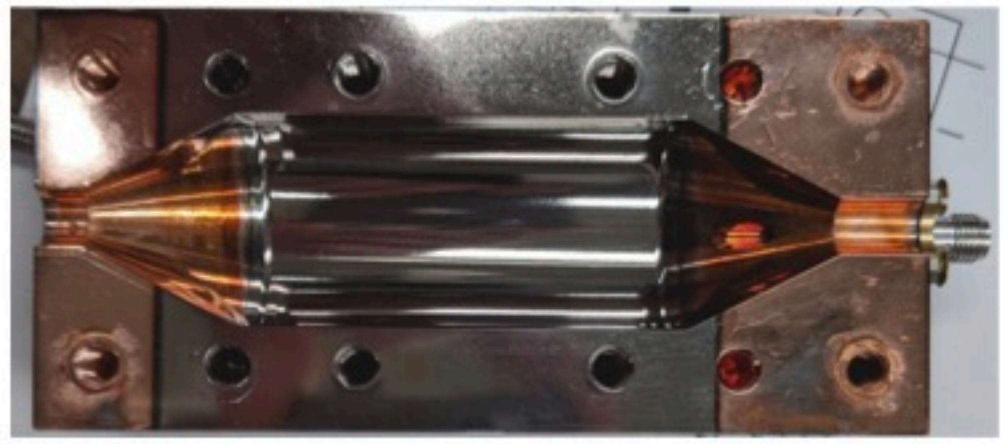

# Q·B²

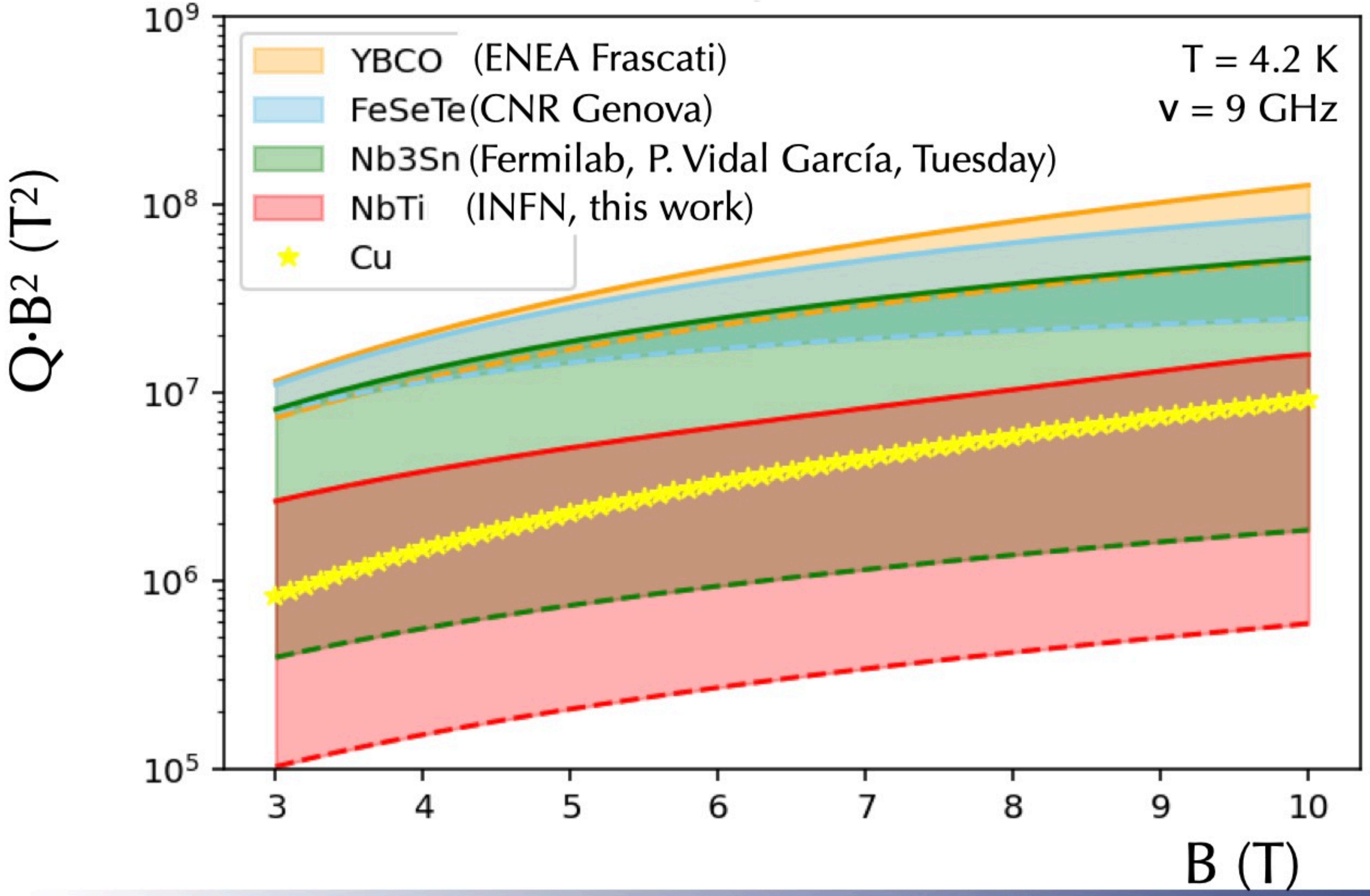

YBCO (ENEA Frascati)
FeSeTe(CNR Genova)
Nb3Sn (Fermilab, P. Vidal García, Tuesday)
NbTi (INFN, this work)
Cu
T = 4.2 K
ν = 9 GHz
10⁹
10⁸
10⁷
10⁶
10⁵
3
4
5
6
7
8
9
10
Q·B² (T²)
B (T)


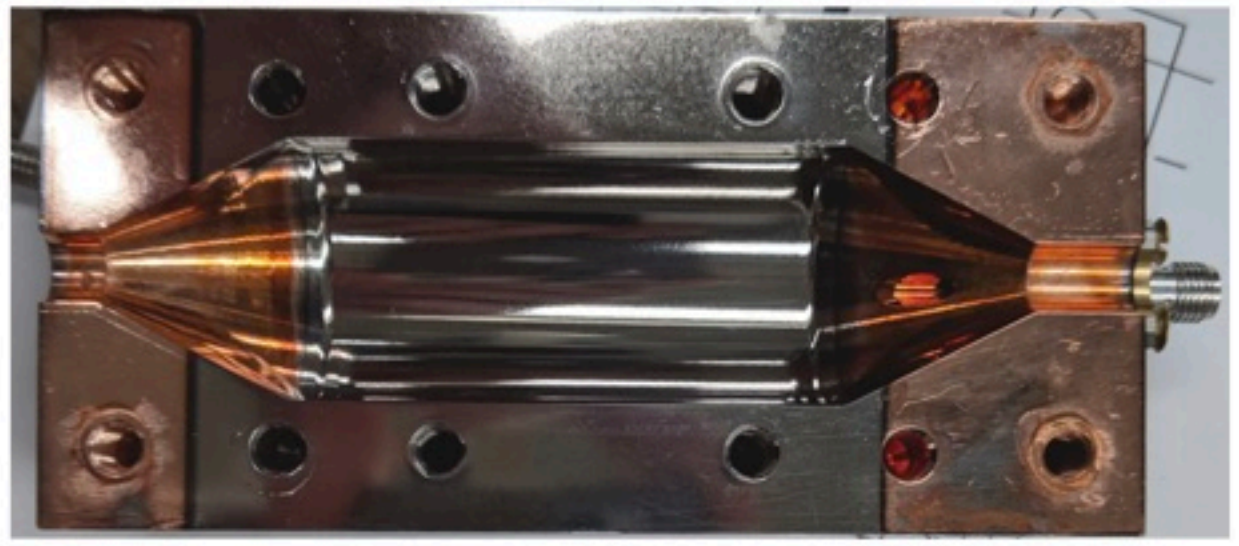

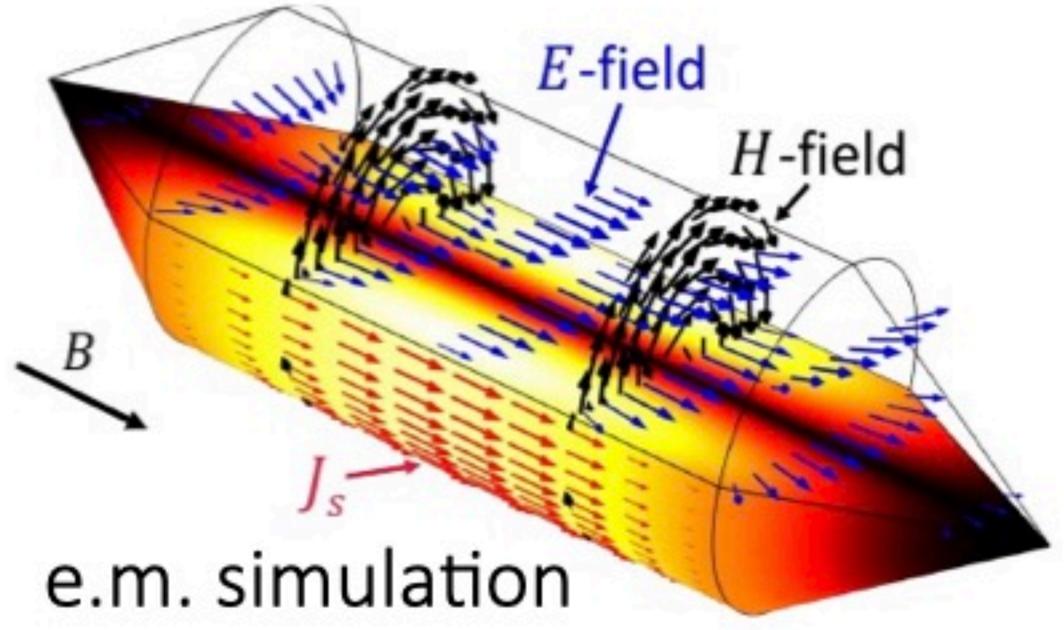

E-field
H-field
B
Js
e.m. simulation

# Summary

- dc field: totally different paradigma for RF superconductivity
- to predict/estimate haloscope performances, vortex physics is required…
- … but it's not sufficient: geometry plays a major role
- the usual (for vortex physics) rule "strong pinning = good, weak pinning = bad" does not necessarily applies.
- … so that all features (pinning, $\lambda$, geometry, operating frequency, …) should be estimated
- … as well as the design of the haloscope (cones: are they *really* better if superconducting?)

# Summary

- dc field: totally different paradigma for RF superconductivity
- to predict/estimate haloscope performances, vortex physics is required…
- … but it's not sufficient: geometry plays a major role
- the usual (for vortex physics) rule "strong pinng = good, weak pinning = bad" does not necessarily applies.
- all features (pinning, λ, geometry, operating frequency, …) should be estimated
- … as well as the design of the haloscope (cones: are they *really* better if superconducting?)

**Thank you for your attention!**